Electronic Supplementary Material (ESI) for Inorganic Chemistry Frontiers.

SUPPORTING INFORMATION

Supporting Information for:

Self-assembled ruthenium and osmium nanosystems display potent anticancer profile by interfering with metabolic activity

Mickaël Marloye,[a] Haider Inam,[b] Connor J. Moore,[b] Tyler R. Mertens,[c] Aude Ingels,[d] Marilin Koch,[f] Michal O. Nowicki,[f] Véronique Mathieu,[d,e] Justin R. Pritchard,[b] Samuel G. Awuah,[c] Sean E. Lawler,[f] Franck Meyer,[a] François Dufrasne,[a] Gilles Berger[a,f,*]

*Author for correspondence

[a] Dr. Mickaël Marloye, Prof. Dr. Franck Meyer, Prof. Dr. François Dufrasne, Prof. Dr. Gilles Berger, Microbiology, Bioorganic & Macromolecular Chemistry, Faculté de Pharmacie, Université libre de Bruxelles (ULB), Boulevard du Triomphe, 1050 Brussels, Belgium. E-mail: gilles.berger@ulb.be

[b] Inam Haider, Connor J. Moore, Prof. Dr. Justin R. Pritchard, Department of Biomedical Engineering, Pennsylvania State University, University Park, PA 16802, USA.

[c] Dr. Tyler R. Mertens, Prof. Dr. Samuel G. Awuah, Department of Chemistry, University of Kentucky, Lexington, KY 40506, USA.

[d] Dr. Aude Ingels, Prof. Dr. Véronique Mathieu, Department of Pharmacotherapy and Pharmaceutics, Faculté de Pharmacie, Université libre de Bruxelles (ULB), Boulevard du Triomphe, 1050 Brussels, Belgium.

[e] Prof. Dr. Véronique Mathieu, ULB Cancer Research Center (UCRC), Université libre de Bruxelles (ULB), 1050 Brussels, Belgium.

[f] Dr. Marilin Koch, Dr. Michal O. Nowicki, Prof. Dr. Sean Lawler, Prof. Dr. Gilles Berger, Harvey Cushing Neuro-Oncology Laboratories, Department of Neurosurgery, Brigham and Women's Hospital, Harvard Medical School, Boston, MA 02115, USA.

Table of Contents

General chemistry methods

All non-aqueous reactions were run in oven-dried glassware under a positive pressure of argon, with exclusion of moisture from reagents and glassware using standard techniques for manipulating air-sensitive compounds. Anhydrous solvents were obtained using standard drying techniques. Unless stated otherwise, commercial grade reagents were used without further purification. Reactions were monitored by analytical thin-layer chromatography (TLC) performed on aluminum plates coated with silica gel F254. Visualization of the chromatogram was performed by UV absorbance, aqueous ninhydrin, iodine, or aqueous potassium permanganate. Flash chromatography was performed on 230-400 mesh silica gel with the indicated solvent systems. Infrared spectra were recorded on a IRAffinity-1 Shimadzu FT-IR spectrometer and are reported in reciprocal centimeters (cm-1). Routine nuclear magnetic resonance spectra were recorded on JEOL 400 MHz and 600 MHz spectrometers. Chemical shifts for 1H-NMR are reported in parts per million from tetramethylsilane (TMS), using the residual solvent resonance (CHCl3 (δ 7.27), CHD2SOCD3 (δ 2.50) and CHD2OD (δ 3.31). Data are reported as follows: chemical shift, integration, multiplicity (s = singlet, d = doublet, t = triplet, q = quartet, qn = quintet, m = multiplet and br = broad), and coupling constant in Hz. Chemical shifts for 13C-NMR are reported in parts per million from TMS using the central peak of the solvent resonance as the internal standard (CDCl3 (δ 77.23), CD3SOCD3 (δ 39.51), and CD3OD (δ 49.00)). All 13C-NMR spectra were obtained with complete proton decoupling. High-resolution mass spectrometry spectra were recorded on a MS QTOF-6520 Agilent. UV-Vis Spectra were recorded on a Shimadzu UV-1800.

Synthetic procedures and characterization data

Synthesis of [Ru (η^6-p-cym) Cl_2]$_2$

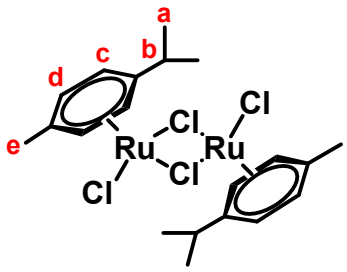

$C_{20}H_{28}Cl_4Os_2$
Mr = 612.39 g/mol

This compound was synthesized according to the following procedure.[1] An ethanolic solution of $RuCl_3.3H_2O$ (1.9 mmol) and α–phellandrene (10 equiv., 19 mmol) was refluxed overnight under argon. The reaction mixture was concentrated under vacuum; a red solid was filtered and washed with Et_2O to afford the desired product in 92 % yield. **^{1}H NMR** (400 MHz, $CDCl_3$): δ (ppm) 5.47 (Hc, d, *J* = 10.4 Hz, 2H), 5.34 (Hd, d, *J* = 10.2 Hz, 2H), 2.91 (Hb, hept, *J* = 6.4 Hz, 1H), 2.15 (He, s, 3H), 1.26 (Ha, d, *J* = 6.7 Hz, 6H).

Synthesis of [Os (η^6-p-cym) Cl_2]$_2$

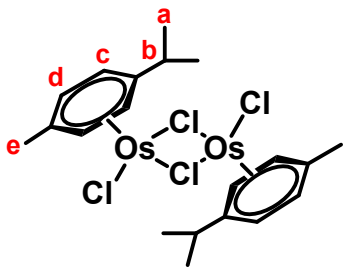

$C_{20}H_{28}Cl_4Os_2$
Mr = 790.71 g/mol

This compound was synthesized according to the following procedure.[2] Briefly, a solution of $OsCl_3.3H_2O$ (1.4 mmol) and α–phellandrene (10 equiv., 14 mmol) in EtOH was refluxed overnight under argon. The reaction medium was then concentrated under vacuum; a yellow solid was filtered off and washed with Et_2O to afford the desired product in 84 % yield. **^{1}H NMR** (400 MHz, $CDCl_3$): δ (ppm) 6.08 (H_c, d, *J* = 10.2 Hz, 2H), 5.97 (H_d, d, *J* = 10.2 Hz, 2H), 2.85 (H_b, hept, *J* = 6.3 Hz, 1H), 2.33 (H_e, s, 3H), 1.26 (H_a, d, *J* = 6.8 Hz, 6H).

Synthesis of Ru[(η^6-p-cym)(phen)Cl]PF$_6$

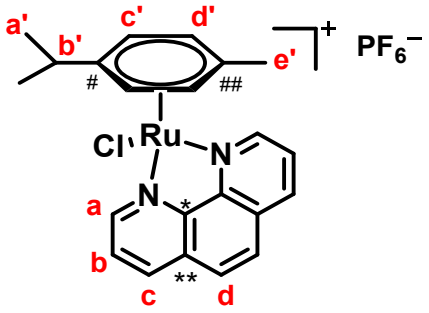

$C_{23}H_{25}ClN_2RuPF_6$
Mr = 595.91 g/mol

This compound was synthesized according to the following procedure.[3] A solution of 1,10-phenanthroline.H_2O (phen, 2 equiv; 0.16 mmol) in 1 mL MeOH was added to a solution of $[(\eta^6\text{-}p\text{-cym})RuCl_2]_2$ (0.08 mmol) in 3 mL MeOH, and the mixture was stirred at reflux for 3 h under argon. A solution of NH_4PF_6 (3 equiv, 0.24 mmol) in 2 mL of MeOH was then added and the solvent volume was reduced to 2 mL on a rotary evaporator. The forming yellow solid was recovered by filtration, washed with cold EtOH and Et_2O, and dried under vacuum to afford the desired product in 87 % yield.

^{1}H NMR (400 MHz, DMSO-d_6): δ (ppm) 9.89 (H_a, d, J = 6.8 Hz, 2H), 8.89 (H_c, d, J = 7.6 Hz , 2H), 8.26 (H_d, s, 2H), 8.15-8-11 (H_b, mult, 2H), 6.30 ($H_{c'}$, d, J = 9.6 Hz, 2H), 6.07 ($H_{d'}$, d, J = 9.6 Hz, 2H), 2.61 ($H_{b'}$, hept, J = 6.4 Hz, 1H), 2.13 ($H_{e'}$, s, 3H), 0.91 ($H_{a'}$, d, J = 6.4 Hz, 6H). **^{13}C NMR** (101 MHz, DMSO-d_6) : δ (ppm) 156.4 (C_a), 145.6 (C*), 139.3 (C_c), 130.6 (C**) 128.0 (C_d), 126.9 (C_b), 104.6 (C$^{\#}$), 103.1 (C$^{\#\#}$), 86.4 ($C_{c'}$), 84.3 ($C_{b'}$), 30.9 ($C_{b'}$), 22.2 ($C_{a'}$), 18.0 ($CH_{e'}$).

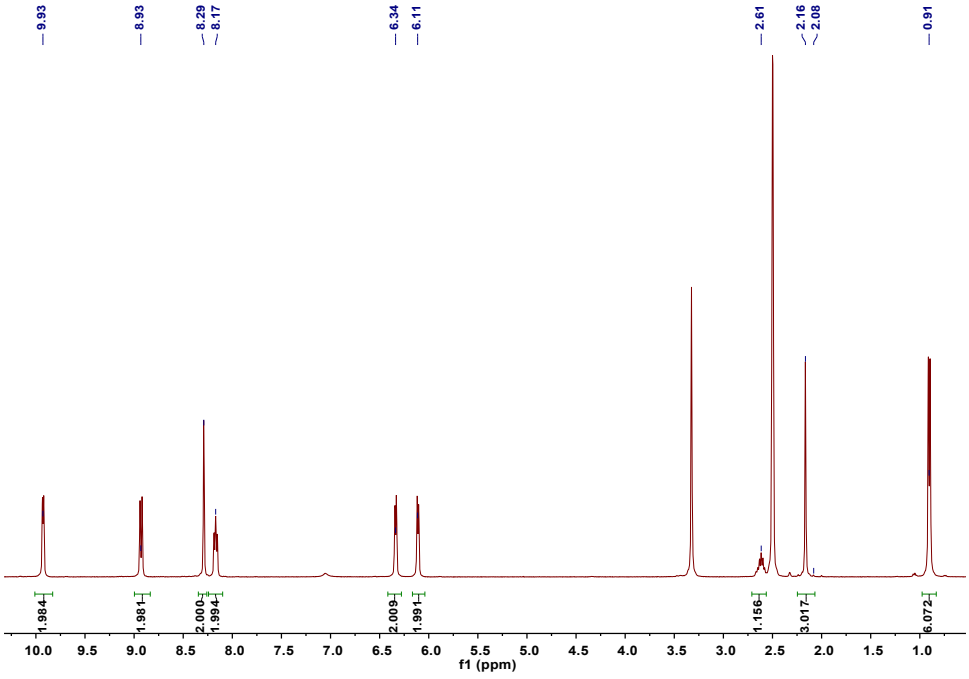

Figure S1. ^{1}H NMR spectrum of RuPhen complex.

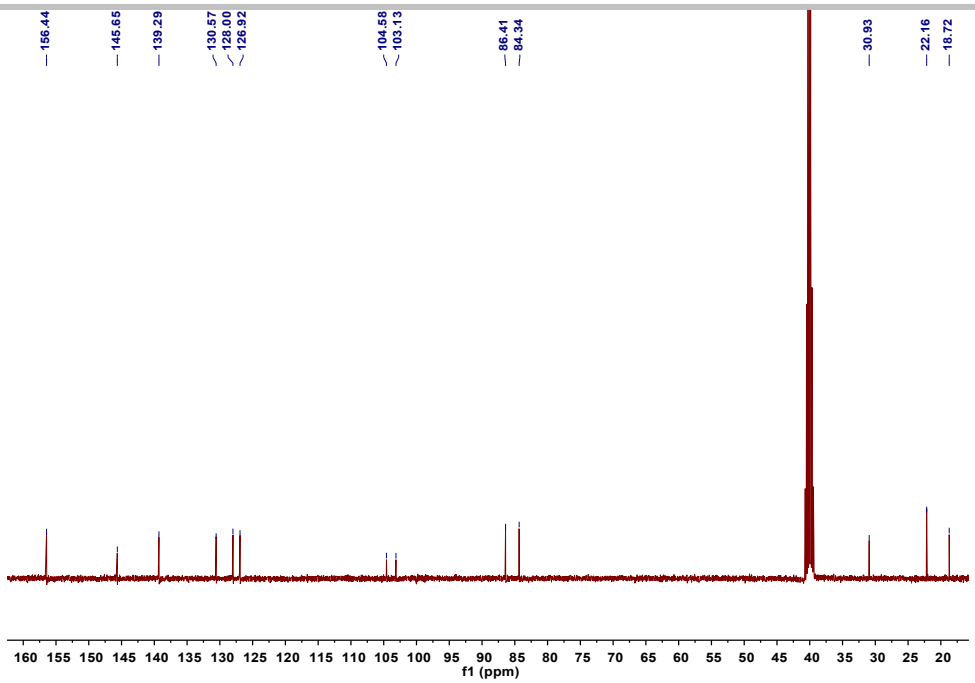

Figure S2. ^{13}C NMR spectrum of RuPhen complex.

Synthesis of $[Os(\eta^6\text{-p-cym})(phen)Cl]PF_6$

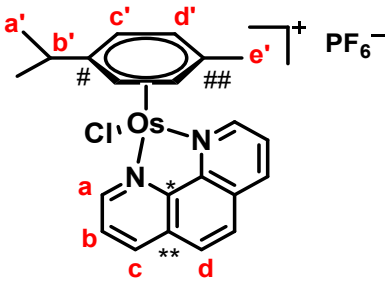

$C_{23}H_{25}ClN_2OsPF_6$
Mr = 685.07 g/mol

This compound was synthesized according to the following procedure.[4] A solution of 1,10-phenanthroline.H_2O (phen, 2 equiv.; 0.13 mmol) in 1 mL MeOH was added to a solution of $[(\eta^6\text{-}p\text{-cym})OsCl_2]_2$ (0.06 mmol) in 3 mL MeOH, and the mixture was stirred at reflux overnight under argon. The solution was filtered through a glass wool plug, and the solvent volume was reduced to 2 mL on a rotary evaporator. A solution of NH_4PF_6 (31 mg, 0.19 mmol) in 2 mL MeOH was added, and the solvent volume was reduced to 2 mL under reduced pressure. The residue was sonicated in ethanol to give a bright yellow suspension. The yellow solid was recovered by filtration, washed with cold EtOH and Et_2O, and dried to afford the desired product in 81 % yield.

^{1}H NMR (400 MHz, DMSO-d_6): δ (ppm) 9.87 (H_a, d, J = 8.5 Hz , 2H), 8.94 (H_c, d, J = 8.3 Hz, 2H), 8.34 (H_d, s, 2H), 8.17-8.13 (Hb, mult, 2H), 6.57 ($H_{c'}$, d, J = 10.2 Hz, 2H), 6.31 ($H_{d'}$, d, J = 10.2 Hz, 2H), 2.33 ($H_{b'}$, hept, J = 6.4 Hz, 1H), 2.22 ($H_{e'}$, s, 3H), 0.84 ($H_{a'}$, d, J = 5.6 Hz, 6H). **^{13}C NMR** (101 MHz, DMSO-D_6) : δ (ppm) 156.3 (C_a), 146.7 (C*), 139.6 (C_c), 130.8 (C**), 128.3 (C_d), 127.5 (C_b), 95.9 ($C^{\#}$), 95.3 ($C^{\#\#}$), 78.0 ($C_{c'}$), 74.8 ($C_{d'}$), 31. ($C_{b'}$), 22.42 ($CH_{a'}$), 18.6 ($CH_{e'}$).

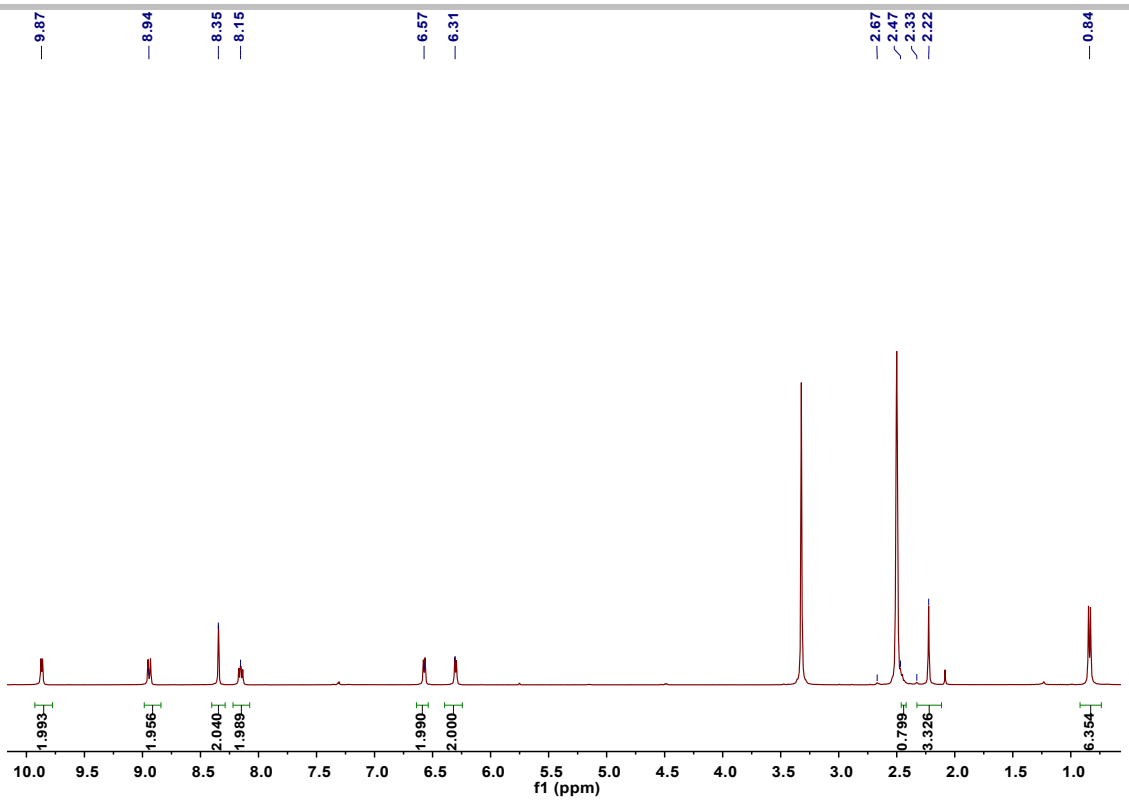

Figure S3. ^{1}H NMR spectrum of OsPhen complex.

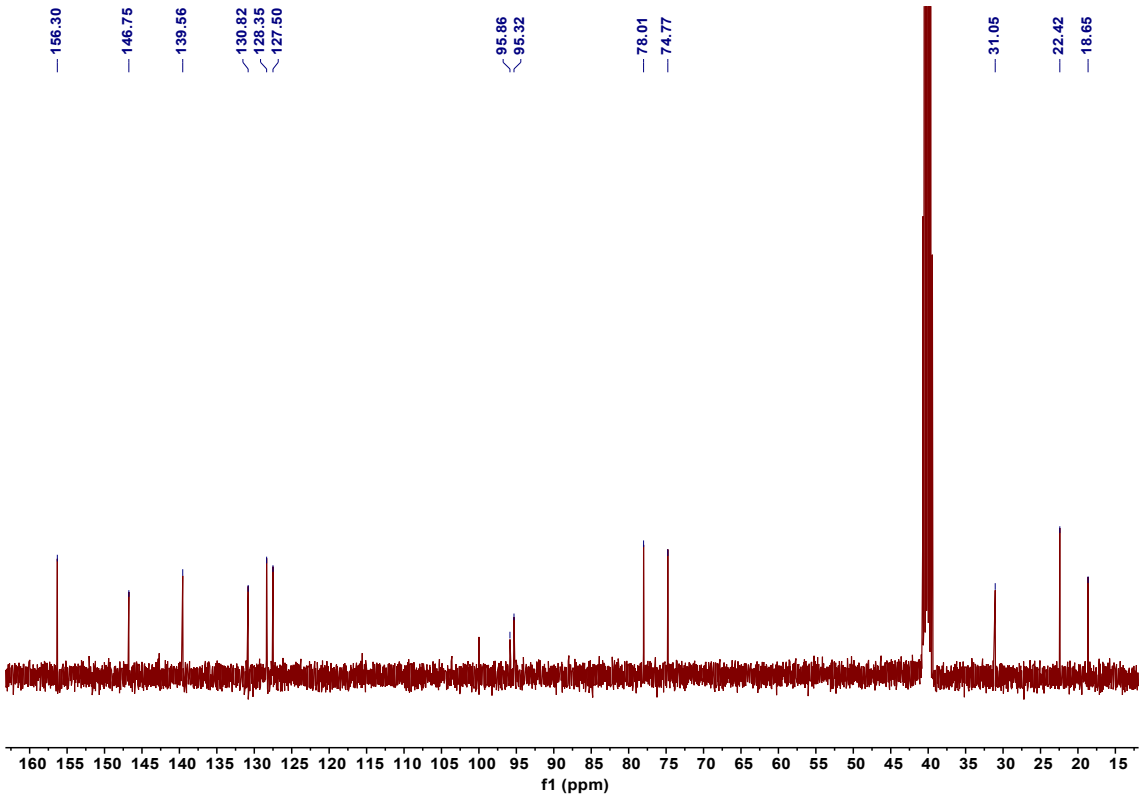

Figure S4. ^{13}C NMR spectrum of OsPhen complex.

Synthesis of L1

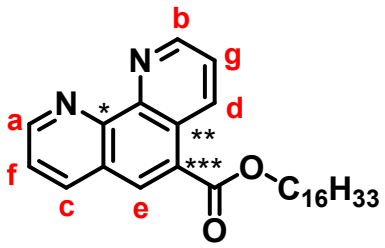

$C_{29}H_{40}N_2O_2$
Mr = 448.64 g/mol

1,10-Phenanthroline-5-carboxylic acid was synthesized according to literature from phenanthroline.H_2O.[5] A solution of 1,10-phenanthroline-5-carboxylic acid (0.67 mmol) and coupling agent HATU (1.2 equiv.; 0.80 mmol) was prepared before the rapid addition of DIPEA (3 equiv.; 2 mmol) in 3 mL DMF and stirred for 1 h. A solution of 1-hexadecanol (1.2 equiv.; 0.80 mmol) was then added to the reaction and stirred for 48 h. The reaction was then transferred into a conical flask before the addition of 100 mL H_2O. The flask stayed at 4 °C for 24 h. A white solid was then filtered and washed several times with H_2O and EtOAc. The residue was dried under reduced pressure to afford the desired product in 68% yield.

^{1}H NMR (400 MHz, $CDCl_3$) : δ (ppm) 9.40 (H_a, dd, J_1 = 7.8 Hz, J_2 = 2.3 Hz, 1H), 9.27 (H_b, dd, J_1 = 8.4 Hz, J_2 = 2.2 Hz, 1H), 9.22 (H_c, dd, J_1 = 8.4 Hz, J_2 = 2.2 Hz, 1H), 8.57 (H_e, s, 1H), 8.33 (H_d, dd, J_1 = 8 Hz, J_2 = 2 Hz , 1H), 7.72-7.67 (H_{fg}, mult, 2H), 4.45 (-CH_2-O-, t, J = 7.2 Hz, 2H), 1.86 (-CH_2-CH_2-O-, quint, J = 5.6 Hz, 2H,), 1.53-1.23 (-CH_2-, mult, 29H, 0.86 (-CH_3, t, J = 5.6 Hz, 3H). **^{13}C NMR** (101 MHz, $CDCl_3$): δ (ppm) 166.3 (C=O), 152.5 (C_a), 150.5 (C_b), 147.7 (C*), 146.2 (C*), 137.4 (C_c), 134.9 (C_d), 131.9 (C_e), 126. (C**), 126.1 (C***), 123.7 (C_{fg}), 65.9 (-CH_2-O-), 32.0 (-CH_2-), 29.8 (-CH_2-), 29.7 (-CH_2-), 29.7 (-CH_2-), 29.7 (-CH_2-), 29.7 (-CH_2-), 29.6 (-CH_2-), 29.4 (-CH_2-), 29.4 (-CH_2-), 28.8 (-CH_2-), 26.2 (-CH_2-), 22.8 (-CH_2-), 14.2 (CH_3). **IR** (cm^{-1}): 2922, 2851, 1716. **ESI-MS** (positive mode) for $C_{29}H_{40}N_2O_2$: calculated m/z 448.3098; found 449.317 $[M-H]^+$ (1.73ppm)

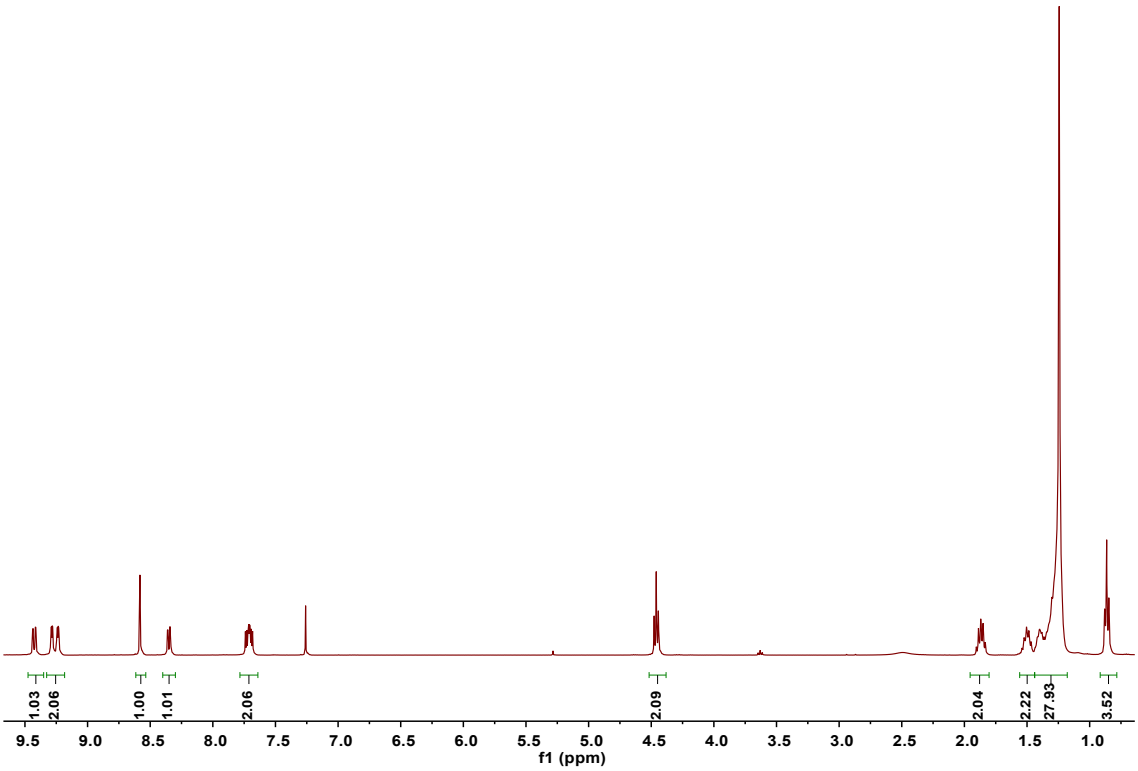

Figure S5. ^{1}H NMR spectrum of compound L1.

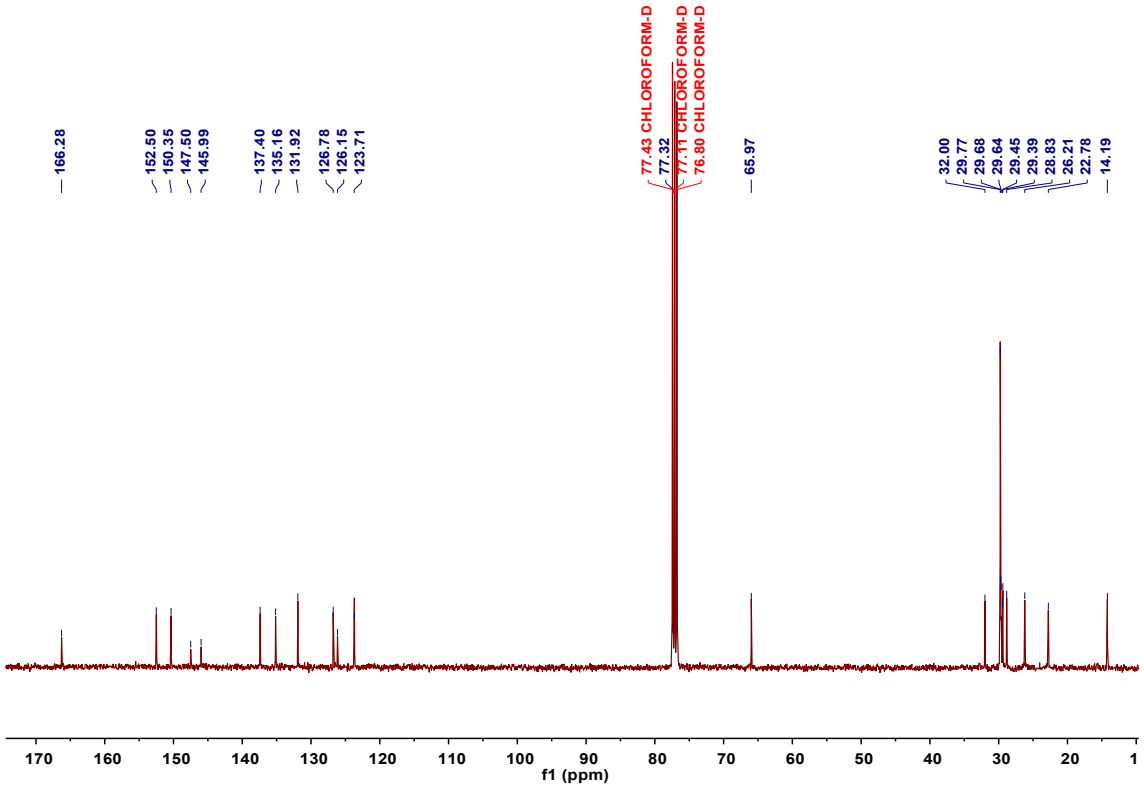

Figure S6. ^{13}C NMR spectrum of compound L1.

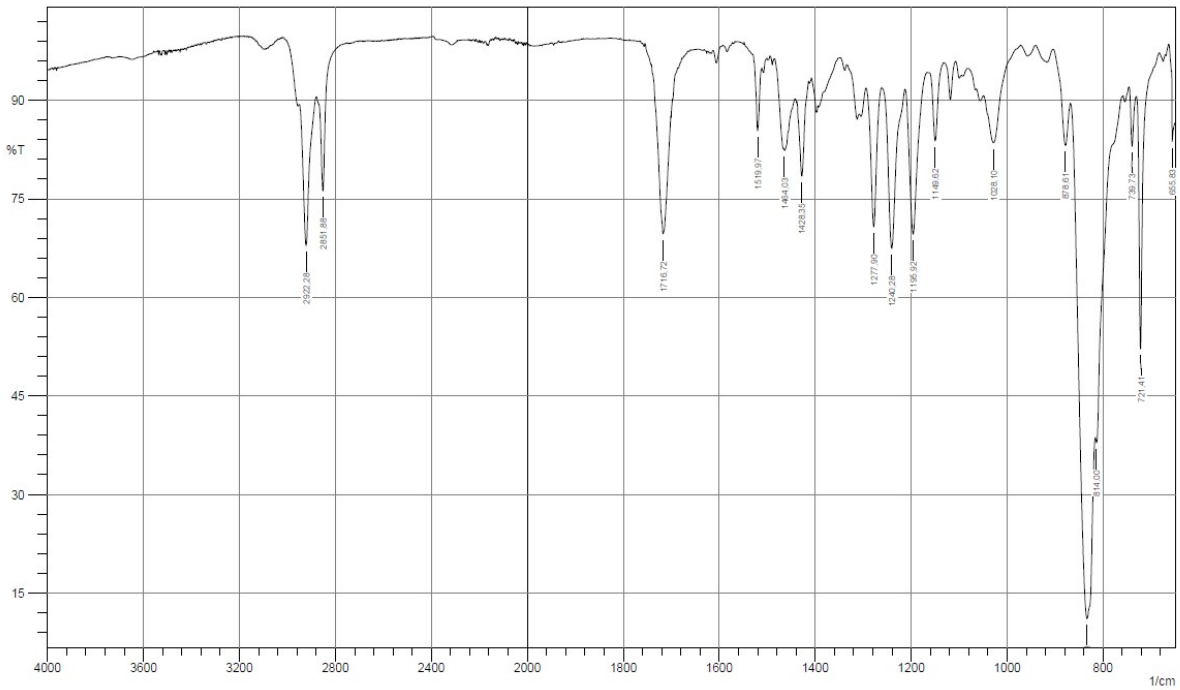

Figure S7. IR spectrum of compound L1.

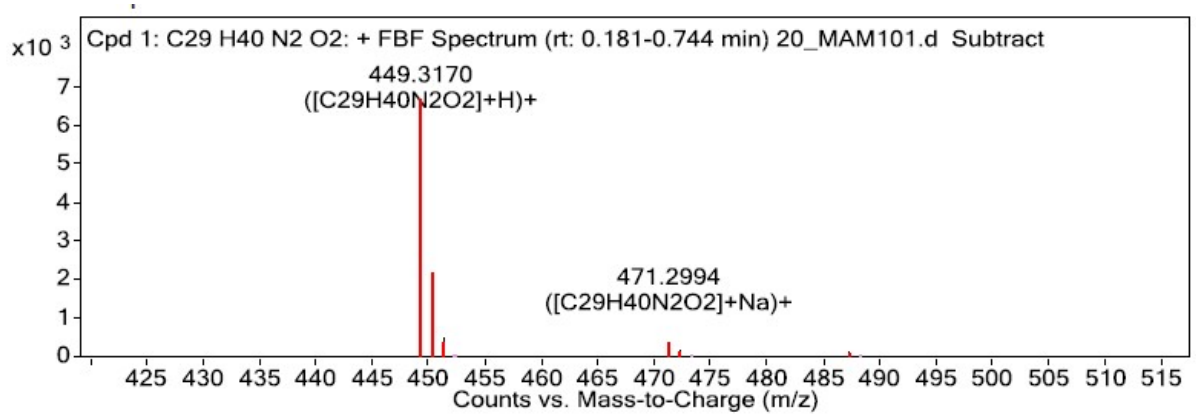

Figure S8. MS spectrum of compound L1.

Synthesis of L2

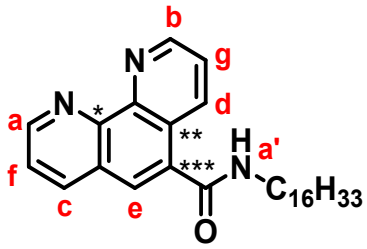

$C_{29}H_{41}ON_3$

Mr = 447.66 g/mol

1,10-Phenanthroline-5-carboxylic acid was synthesized according to literature from Phenanthroline.H_2O. A solution of 1,10-phenanthroline-5-carboxylic acid (0.67 mmol) and HATU (1.2 equiv.; 0.80 mmol) in 3 mL dry DMF was prepared before the addition of DIPEA (3 equiv.; 2 mmol) and stirred for 1 h. A solution of 1-hexadecylamine (1.2 equiv.; 0.80 mmol) was then added to the reaction and stirred for 48 h. The reaction was transferred into a conical flask before the addition of 100 mL water and storage at 4 °C for 24 h. A white solid was recovered and washed several times with H_2O and EtOAc, then dried under reduced pressure to afford the desired product in 73% yield.

^{1}H NMR (400 MHz, DMSO-d_6) : δ (ppm) 9.17 (H_a, dd, J_1 = 8.8 Hz, J_2 = 2.3 Hz, 1H), 9.14 (H_b, dd, J_1 = 8.7 Hz, J_2 = 2.2 Hz, 1H), 8.6 (H_c, dd, J_1 = 8.4 Hz, J_2 = 1.9 Hz, 1H), 8.14 (H_d, dd, J_1 = 8.4 Hz, J_2 = 2 Hz, 1H), 7.79 (H_e, s, 1H), 7.61-7.55 (H_{fg}, mult, 2H), 6.47 ($H_{a'}$, t, J = 5.2 Hz, 1H), 3.59 (-O-CH_2-, q, J = 6.8 Hz, 2H), 1.56 (-CH_2-, quint, J = 6.4 Hz, 4H), 1.38-1.18 (mult, 29H), 0.85 (-CH_3, t, J = 6.4 Hz, 3H). **^{13}C NMR** (101 MHz, DMSO-D_6) : δ (ppm) 167.6 (C=O), 151.5 (C_a), 150.6 (C_b), 146.2 (C*), 146.0 (C*), 137.2 (C_c), 134.6 (C_d), 133.9 (C_e), 127.6 (C**), 126.3 (C**), 126.2 (C***), 124.3 (C_f), 123.9 (C_g), 31.8 (NH-CH_2-), 29.6 (-CH_2-), 29.2 (-CH_2-), 27.0 (-CH_2-), 22.6 (-CH_2-), 14.5 (-CH_3). **IR** (cm^{-1}): 3463, 3274, 2924, 2848, 1631. **ESI-MS** calculated m/z 447.3232; found 448.3318 $[M-H]^+$ (0.78 ppm)

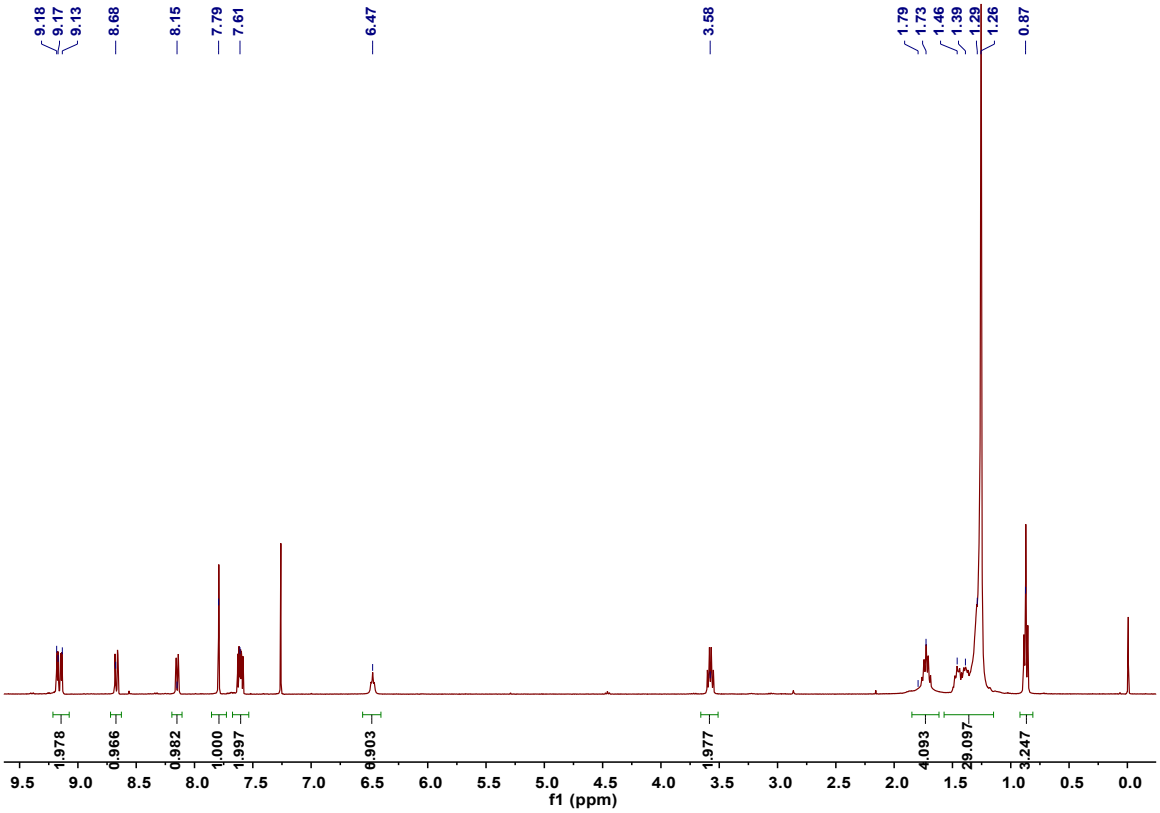

Figure S9. ^{1}H NMR spectrum of compound L2.

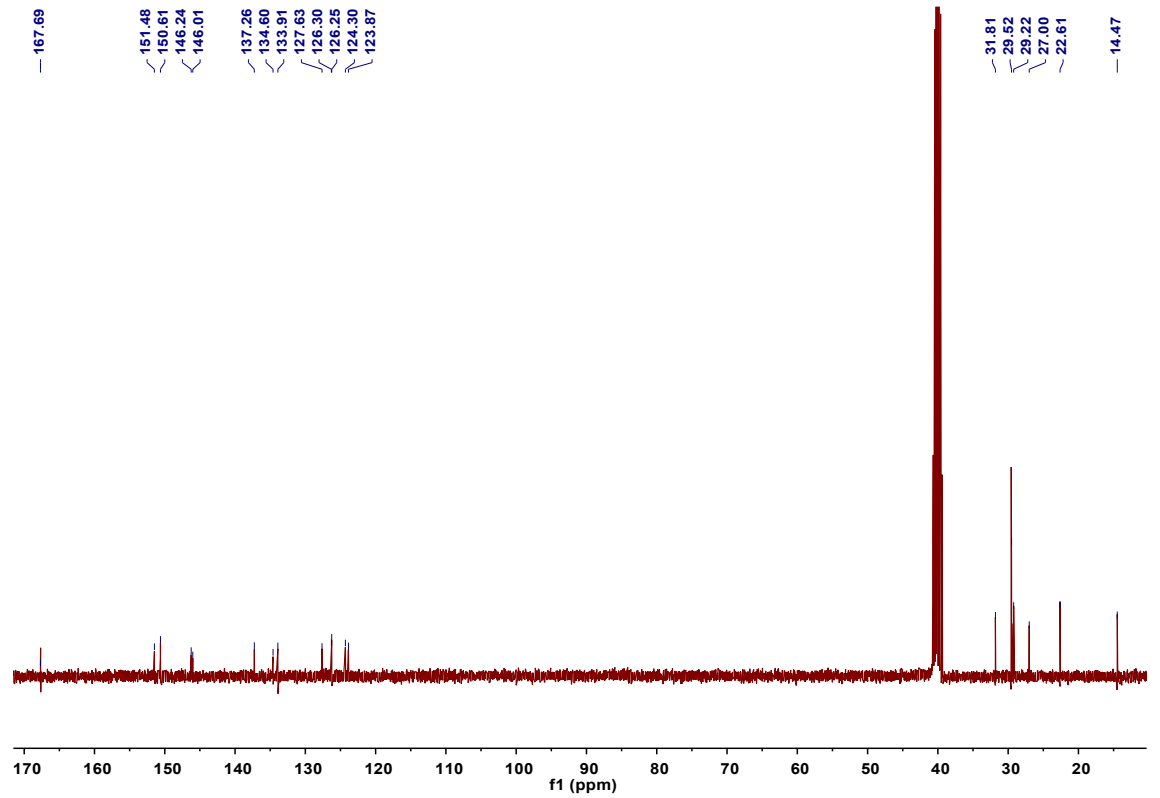

Figure S10. ^{13}C NMR spectrum of compound L2.

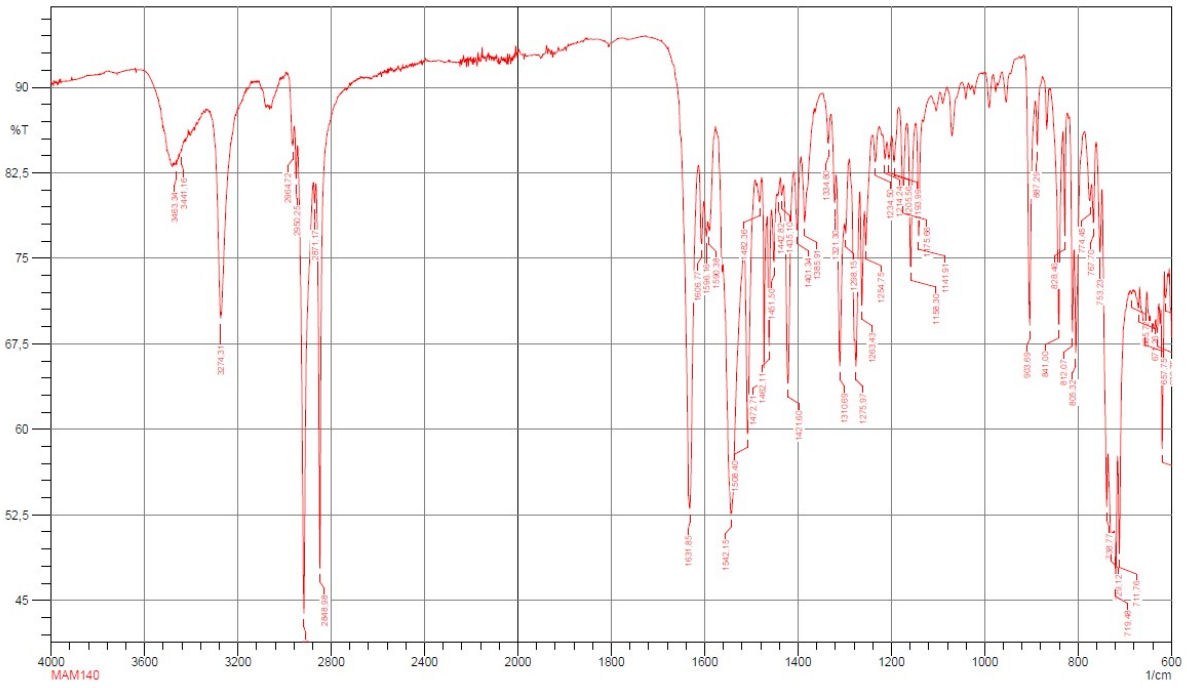

Figure S11. IR spectrum of compound L2.

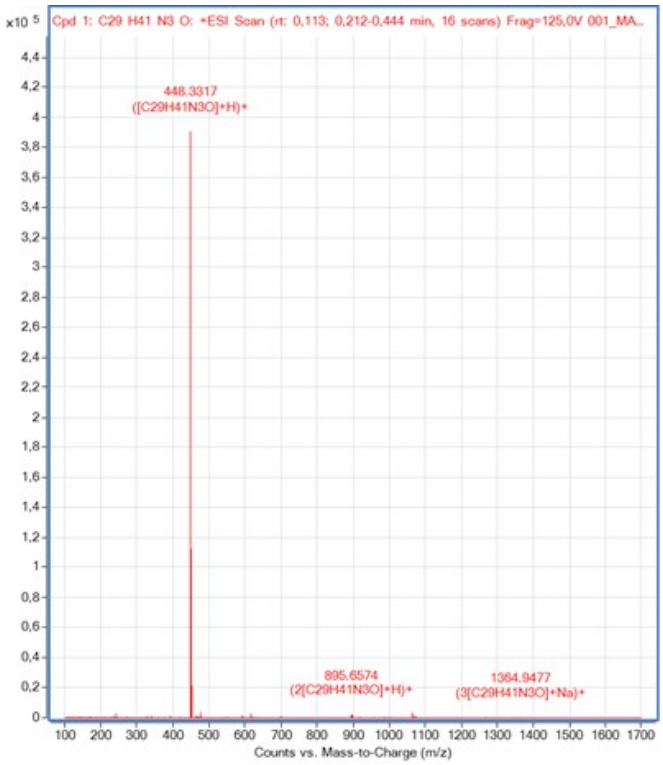

Figure S12. MS spectrum of compound L2.

Synthesis of 1

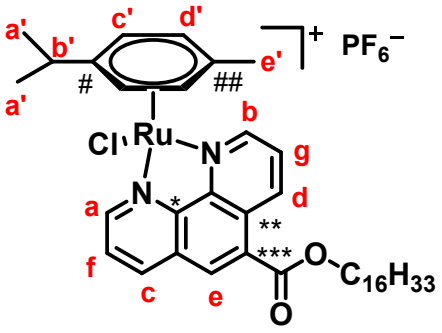

$C_{39}H_{54}ClO_2N_2RuPF_6$

Mr = 864.35 g/mol

A solution of L1 (2 equiv; 0.10 mmol) and $[Ru(\eta^6\text{-}p\text{-cym})Cl_2]_2$ (0.5 mmol) was prepared in 3 mL of $CHCl_3$, and the mixture was refluxed overnight under argon. A solution of NH_4PF_6 (3 equiv; 0.15 mmol) in 1 mL MeOH was added, a yellow solid formed and the reaction was allowed to run for 2 more hours before discarding the supernatant. The yellow residue was then dissolved in CH_2Cl_2, filtered off and evaporated under reduced pressure. The obtained yellow solid was washed with 10 mL Et_2O, sonicated, filtered and dried under reduced pressure to afford the desired product in 89 % yield.

^{1}H NMR (400 MHz, $CDCl_3$) : δ (ppm) 9.86 (H_a, d, *J* = 7.8 Hz, 1H), 9.78 (H_b, d, *J* = 8.4 Hz, 1H), 9.68 (H_c, d, *J* = 10 Hz, 1H), 8.76 (H_e, s, 1H), 8.62 (H_d, d, *J* =, 10Hz), 8.15-8.09 (H_{fg}, mult, 2H), 6.11 (Hc', t, *J* = 11.2 Hz, 2H), 5.88 (Hd', d, *J* = 11.2 Hz, 2H), 4.47 (CH_2-O-, t, *J* = 8.4 Hz, 2H), 2.68 (Hb', hept, *J* = 7.2 Hz, 1H), 2.23 ($H_{e'}$, s, 3H), 1.86 (CH_2-CH_2-O-, quint, *J* = 6.4 Hz, 2H), 1.47-1.25 (CH_2, mult, 29H), 1.00 ($H_{a'}$, dd, J_1 = 1.2 Hz, J_2 = 2.8 Hz ,6H), 0.87 (-CH_3, t, *J* = 6.4 Hz, 3H). **^{13}C NMR** (101 MHz, $CDCl_3$) : δ (ppm) 164.5 (C=O), 157.9 (C_a), 156.1 (C_b), 147.1 (C*), 146.1 (C*), 139.3 (C_c), 137.7 (C_d), 132.3 (C_e), 129.0 (C**), 128.6 (C***), 127.5 (C_f), 127.2 (C_g), 105.6 ($C^{\#}$), 103.9 ($C^{\#\#}$), 86.7 ($C_{c'}$), 84.2 ($C_{d'}$), 66.8 (CH_2-O-), 31.9 (-CH_2-), 31.2 ($C_{b'}$), 29.8 (-CH_2-), 29. (-CH_2-), 29.7 (-CH_2-) , 29.6 (-CH_2-), 29.4 (-CH_2-), 29.4 (-CH_2-), 28.7 (-CH_2-), 26.1 (-CH_2-), 22.8 ($C_{a'}$), 22.1 (-CH_2-), 18.9 ($C_{e'}$), 14.2 (-CH_3). **IR** (cm^{-1}): 2920.3, 2850.9, 1716.7. **ESI-MS** (positive mode) for $RuC_{39}H_{54}N_2O_2Cl$: $[M]^+$, calculated m/z 719.29; found 719.29 $[M]^+$ (0.16 ppm). **HPLC-UV purity:** 98.3 %

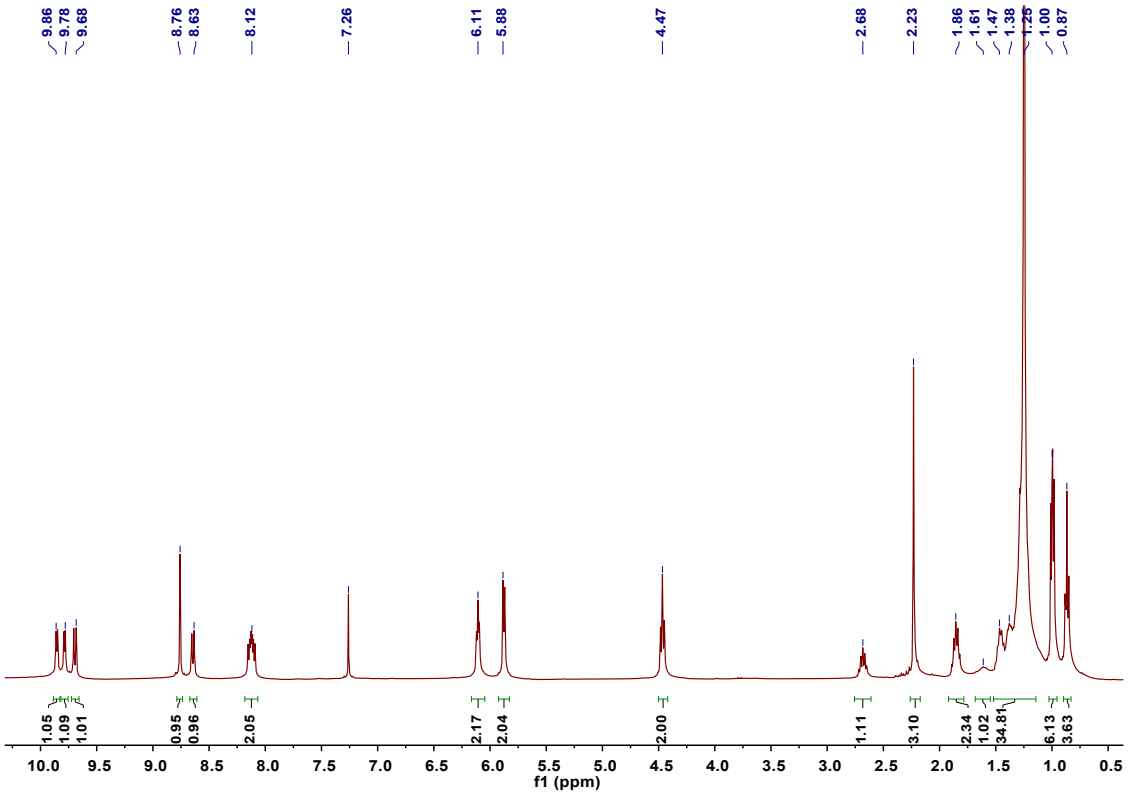

Figure S13. ^{1}H NMR spectrum of complex 1.

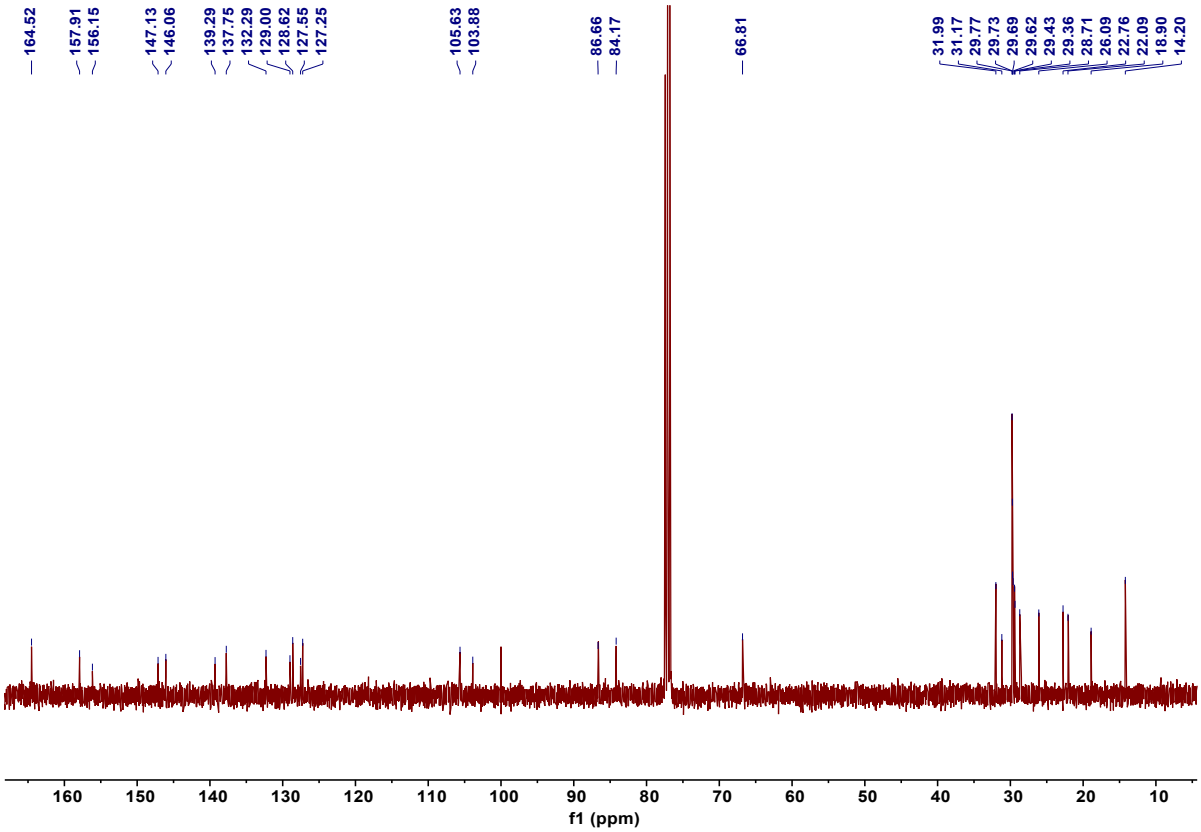

Figure S14. ^{13}C NMR of complex 1.

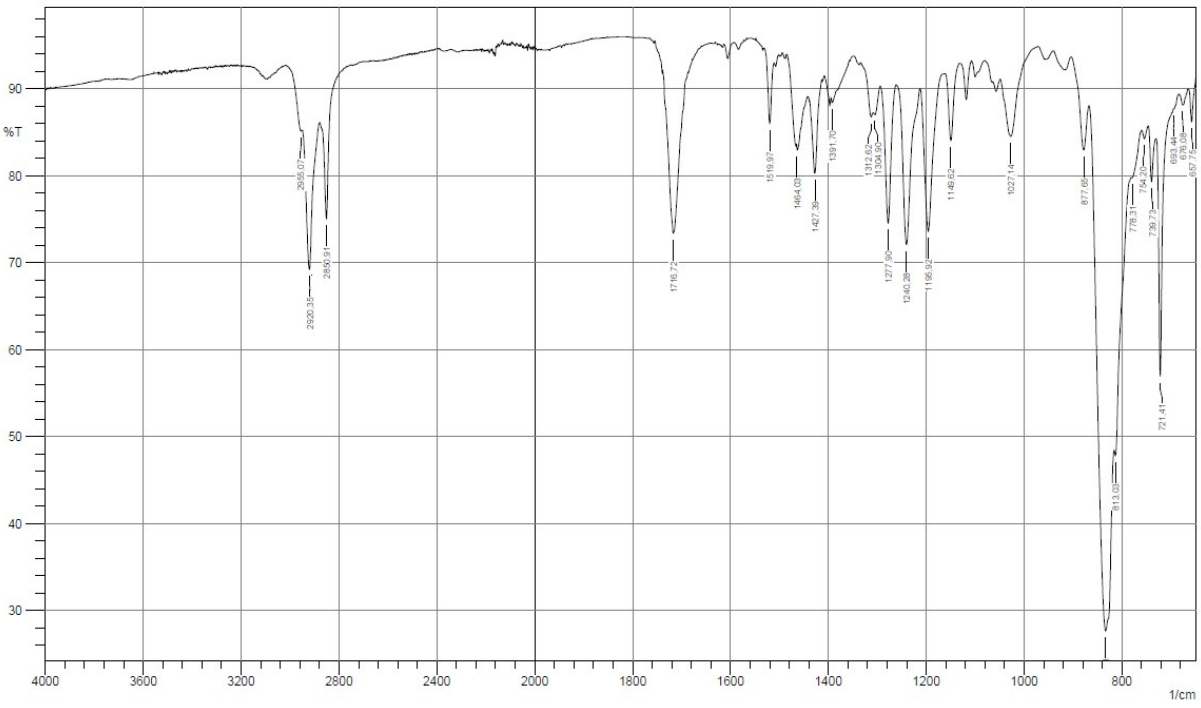

Figure S15. IR spectrum of complex 1.

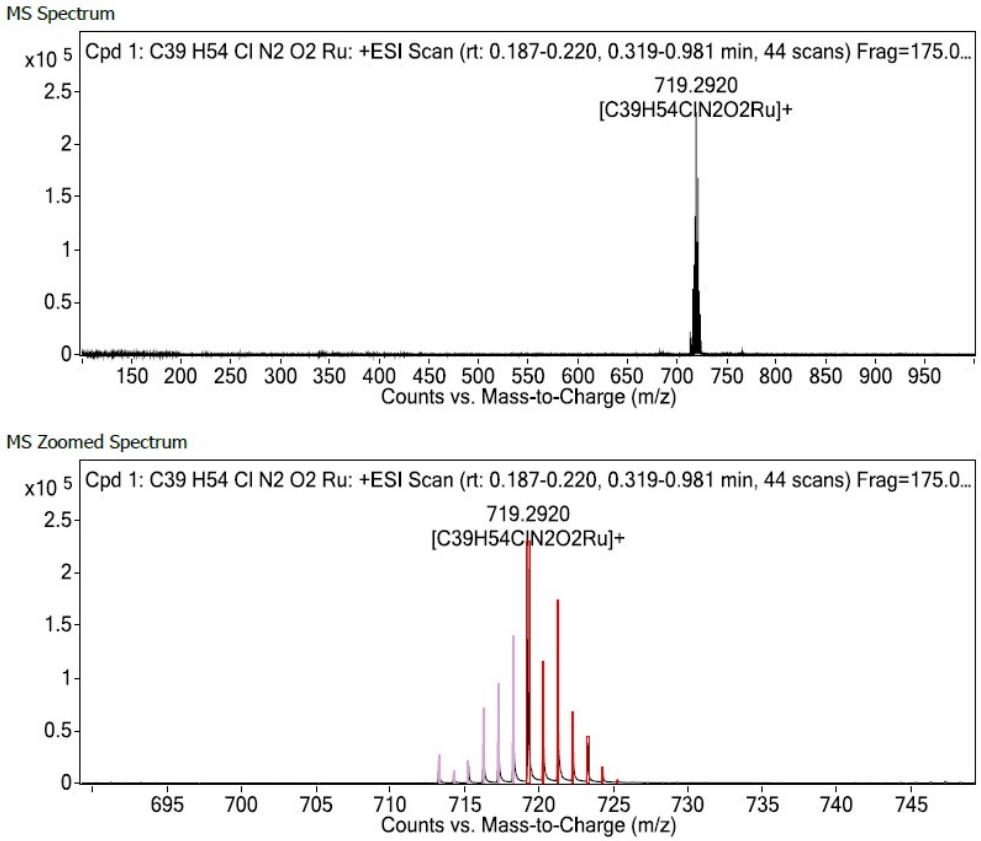

Figure S16. MS spectrum of complex 1.

Synthesis of 2

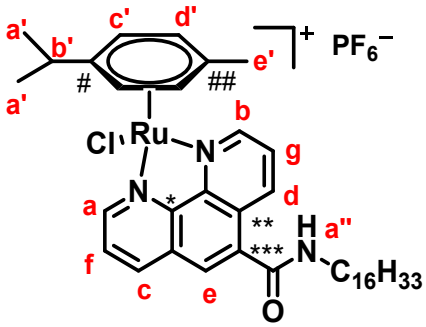

$C_{39}H_{55}ClON_3RuPF_6$
Mr = 863.36 g/mol

A solution of L2 (2 equiv.; 0.08 mmol) and $[Ru(\eta^6\text{-}p\text{-cym})Cl_2]_2$ (0.04 mmol) was prepared in 3 mL of $CHCl_3$, and the mixture was refluxed overnight under argon. A solution of NH_4PF_6 (3 equiv; 0.12 mmol) in 1 mL MeOH was then added. A yellow solid started to precipitate and the reaction was allowed to run for 2 more hours before discarding the supernatant. The yellow residue obtained after solvent evaporation was dissolved in CH_2Cl_2, filtered off and evaporated under reduced pressure. The yellow solid was washed with 10 mL Et_2O, sonicated, filtered and dried under reduced pressure to afford the desired product in 92 % yield.
^{1}H NMR (400 MHz, $CDCl_3$) : δ (ppm) 9.61 (H_a, d, J = 8.4 Hz, 1H), 9.51 (H_b, d, J = 8.4 Hz, 1H), 9.13 (H_c, d, J = 9.6 Hz, 1H), 8.53 (H_d, d, J = 9.6 Hz, 1H), 8.23 (H_e, s, 1H), 7.93-7.89 (H_f, mult, 1H), 7.84-7.81 (H_g, mult, 1H), 7.00 ($H_{a'}$, broad s, 1H), 5.95 ($H_{c'}$, d, J = 12.2 Hz, 2H), 5.76 ($H_{d'}$, d, J = 12.2 Hz, 2H), 3.50 (NH-CH_2, broad s, 2H), 2.67 ($H_{b'}$, hept, J = 4.4 Hz, 1H), 2.15 ($H_{e'}$, s, 3H), 1.68 (NH-CH_2-CH_2-, quint, J = 4.4 Hz, 2H), 1.50-1.25 (CH_2, mult, 30H), 1.0 ($H_{a'}$, dd, J_1 = 5.6 Hz, J_2 = 8.8 Hz, 6H) , 0.86 (-CH_3, t, J = 4.8 Hz, 3H). **^{13}C NMR** (101 MHz, CDCl3) : δ (ppm) 165.8 (C=O), 156.3 (C_a) 154.9 (C_b), 146.2 (C*), 139.3 (C_c), 137.9 (C_d), 134.2 (C_e), 129.5 (C**), 128.9

(C***), 126.9 (C_f), 126.4 (C_g), 105.8 (C#), 103.1 (C##), 86.2 ($C_{c'}$), 84.2 (Cd'), 40.7 (NH-CH_2-), 32.0 (-CH_2-), 31.2 ($C_{b'}$), 29.8 (-CH_2-), 29.4 (-CH_2-), 27.1 (-CH_2-), 22.8 (Ca'), 22.1 (-CH_2-), 18.7 ($C_{e'}$), 14.2 (-CH_3). **IR** (cm^{-1}): 2971.3, 2960.9, 1716.7. **ESI-MS** (positive mode) for $RuC_{39}H_{55}N_3OCl$: $[M]^+$, calculated m/z 718.31; found 718.31 $[M]^+$ (0.05 ppm). **HPLC-UV purity**: 96.9 %

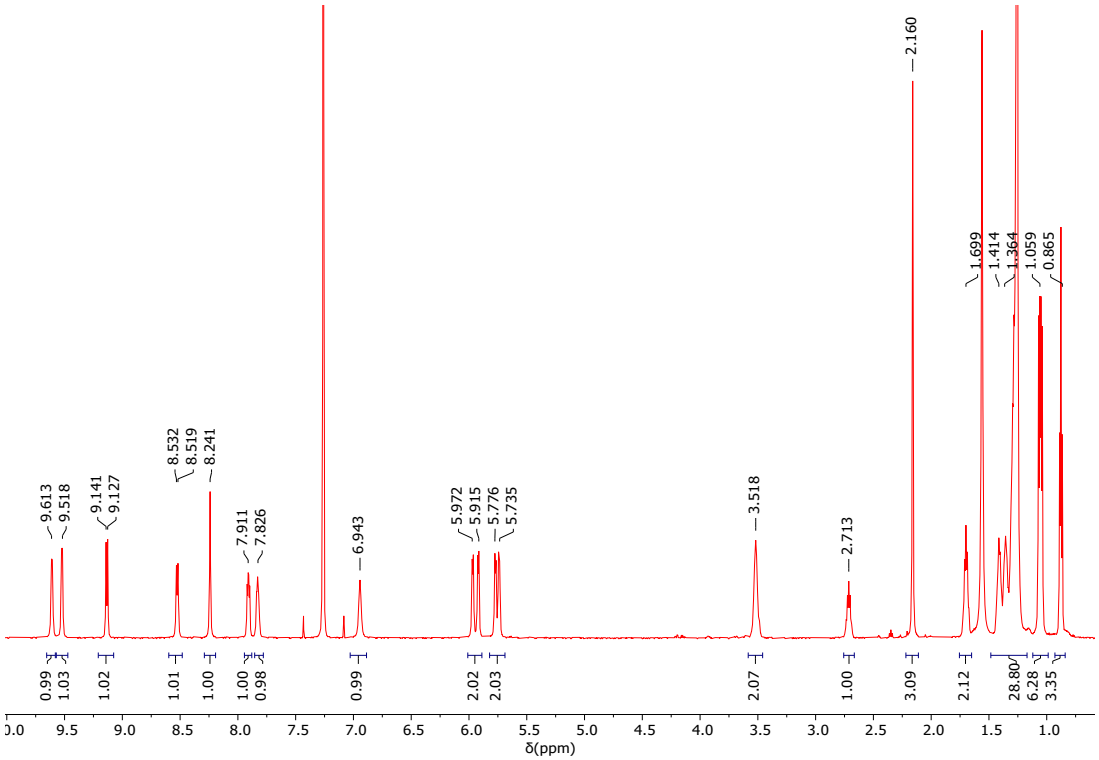

Figure S17. ^{1}H NMR spectrum of complex 2.

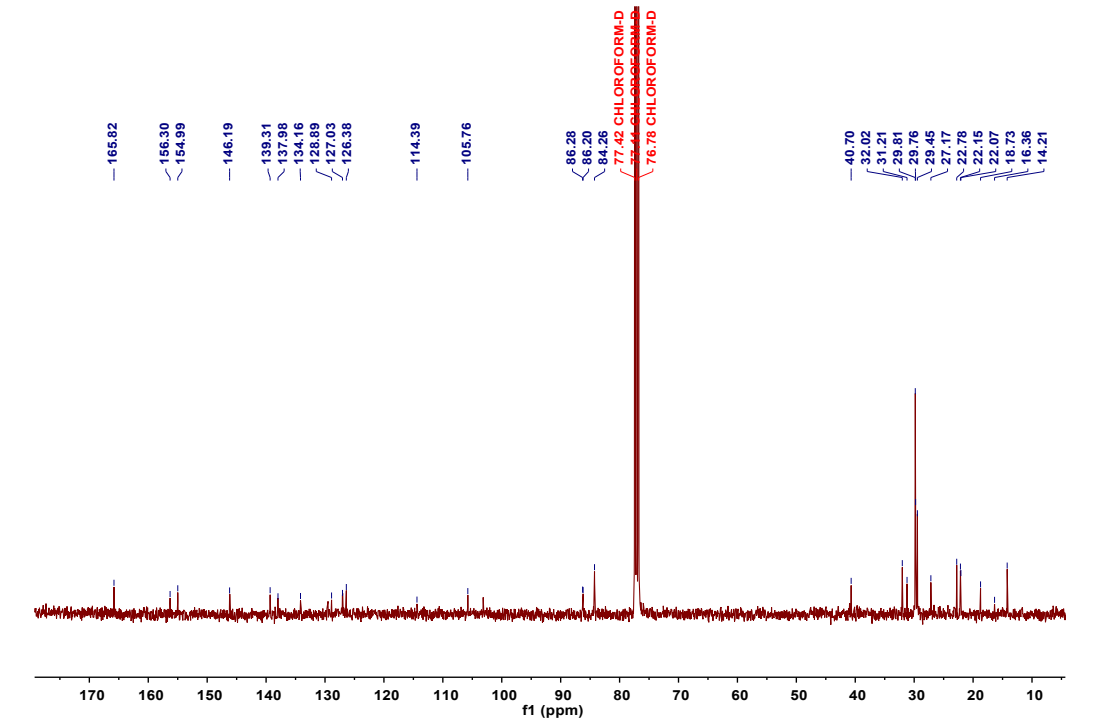

Figure S18. ^{13}C NMR spectrum of complex 2.

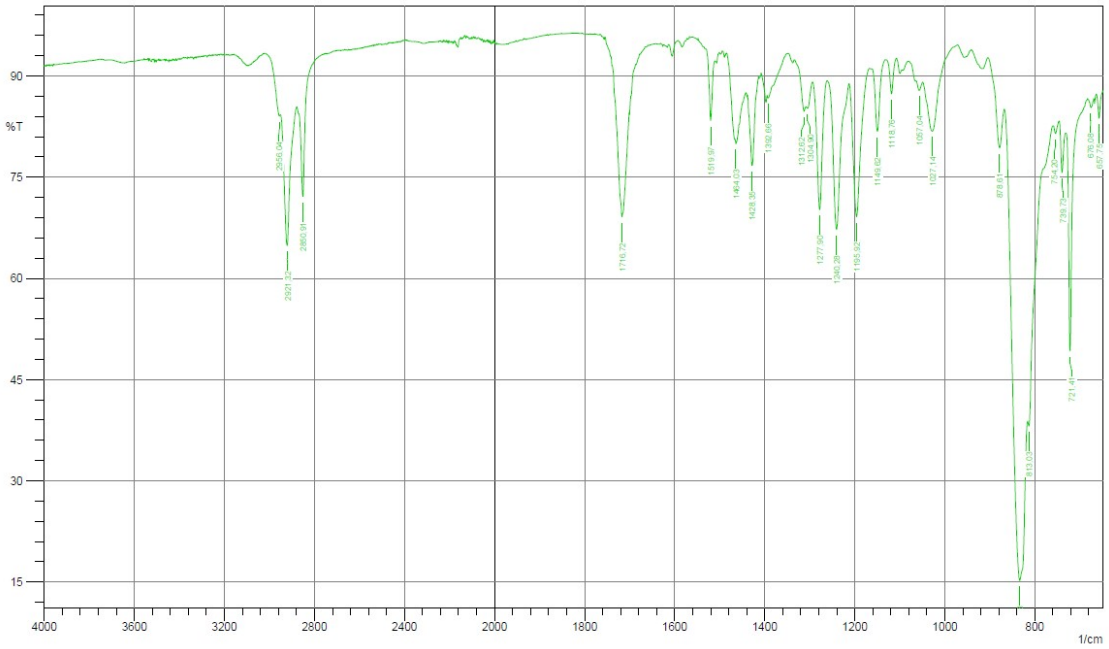

Figure S19. IR spectrum of complex 2

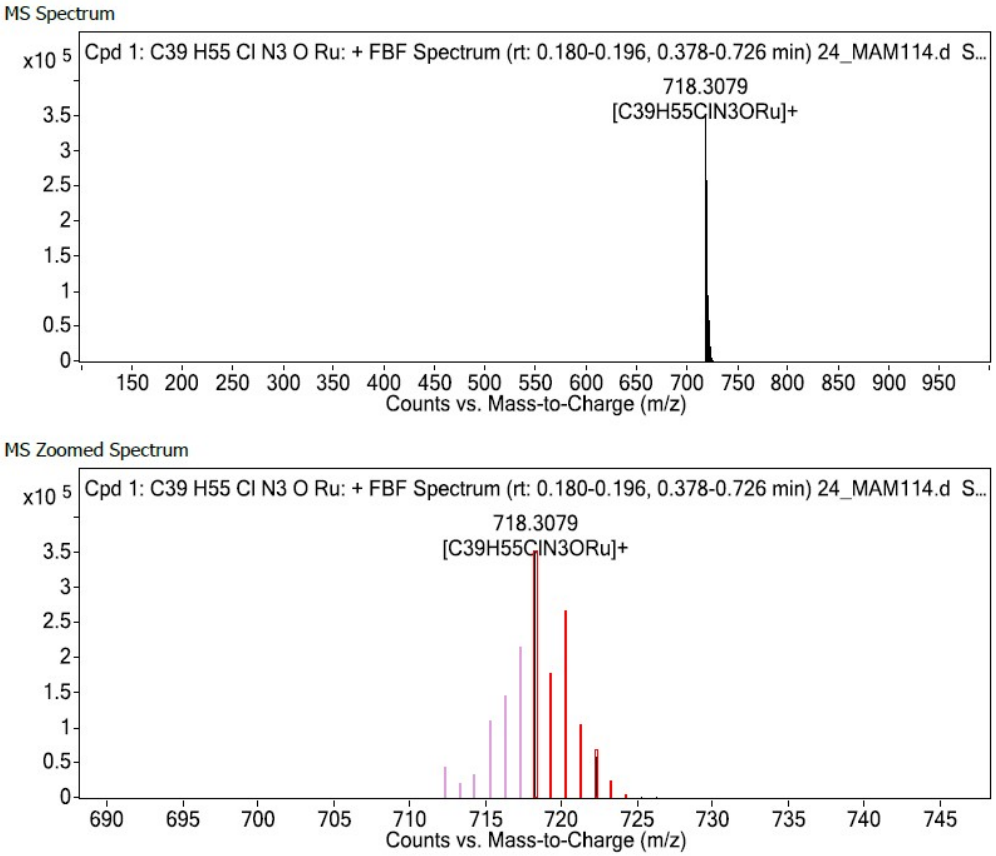

Figure S20. MS spectrum of complex 2.

Synthesis of 3

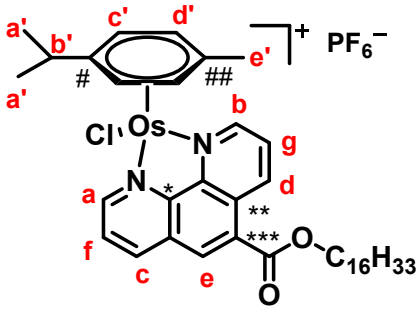

$C_{39}H_{54}ClO_2N_2OsPF_6$

Mr = 953.51 g/mol

A solution of L1 (2 equiv; 0.08 mmol) and $[Os(\eta^6\text{-}p\text{-cym})Cl_2]_2$ (0.04 mmol) was prepared in 3 mL of MeOH and the mixture was refluxed overnight under argon, then added with a solution of NH_4PF_6 (3 equiv; 0.12 mmol) in 1 mL MeOH. A yellow solid formed and the reaction was allowed to run for 2 more hours before discarding the supernatant. The yellow residue obtained after solvent evaporation was dissolved in CH_2Cl_2, filtered off and evaporated under reduced pressure. The resulting yellow solid was washed with 10 mL Et_2O, sonicated, filtered and dried under reduced pressure to afford the desired product in 74 % yield.

^{1}H NMR (400 MHz, $CDCl_3$) : δ (ppm) 9.77 (H_a, dd, J_1 = 9.8 Hz, J_2 = 2.4 Hz, 1H), 9.70-9.67 (H_{bc}, mult, 3H), 8.82 (H_e, s, 1H), 8.65 (H_d, dd, J_1 = 9.6 Hz, J_2 = 2.4 Hz, 1H), 8.12-8.05 (H_{fg}, mult, 2H), 6.31 ($H_{c'}$, dd, J_1 = 11.8 Hz, J_2 = 4.2 Hz, 2H), 6.04 ($H_{d'}$, dd, J_1 = 11.8 Hz, J_2 = 4.2 Hz, 2H), 4.48 (-O-CH_2, t, J = 7.6 Hz, 2H), 2.51 ($H_{b'}$, hept, J = 7.6 Hz, 1H), 2.27 ($H_{e'}$, s, 3H), 1.86 (O-CH_2-CH_2-,quint, J = 6.8 Hz, 2H), 1.51-1.24 (mult, 30H), 0.92 ($H_{a'}$, dd, J_1 = 4.4 Hz, J_2 = 6.8 Hz, 6H), 0.86 (-CH_3, t, J = 7 Hz, 3H). **^{13}C NMR** (101 MHz, $CDCl_3$) : δ (ppm) 164.5 (C=O), 157.7 (C_a), 155.8 (C_b), 148.2 (C*), 147.3 (C*), 139.4 (C_c), 138.1 (C_d), 132.6 (C_e), 129.3 (C**), 128.9 (C**), 128. (C***), 127.8 (C_f), 127.6 (C_g), 96.9 (C#), 96.6 (C##), 78.3 ($C_{c'}$), 74.7 ($C_{d'}$), 66.9 (-O-CH_2-), 32.1 (-CH_2-), 31.4 ($C_{b'}$), 29.8 (-CH_2-), 29.8 (-CH_2-), 29.8 (-CH_2-), 29.7 (-CH_2-), 29.5 (-CH_2-), 29.4 (-CH_2-), 26.2 (-CH_2-), 22.8 (-CH_2-), 22.4 ($C_{a'}$) , 22.3 (-CH_2-), 18.8 ($C_{e'}$), 14.3 (-CH_3). **IR** (cm^{-1}): 2922.2, 2852.8, 1717.1. **ESI-MS** (positive mode) for $OsC_{39}H_{54}N_2O_2Cl$: $[M]^+$, calculated m/z 809.35; found 809.35 $[M]^+$ (0.08 ppm). **HPLC-UV purity:** 98.1 %

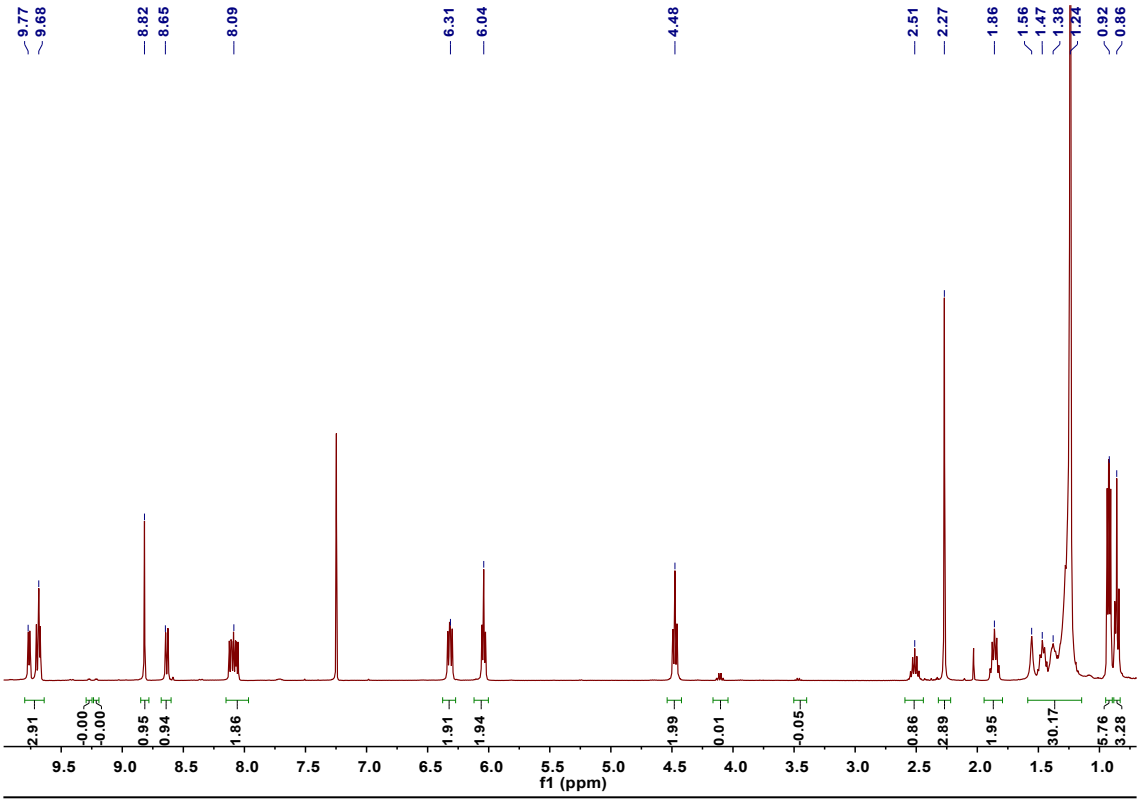

Figure S21. ^{1}H NMR spectrum of complex 3.

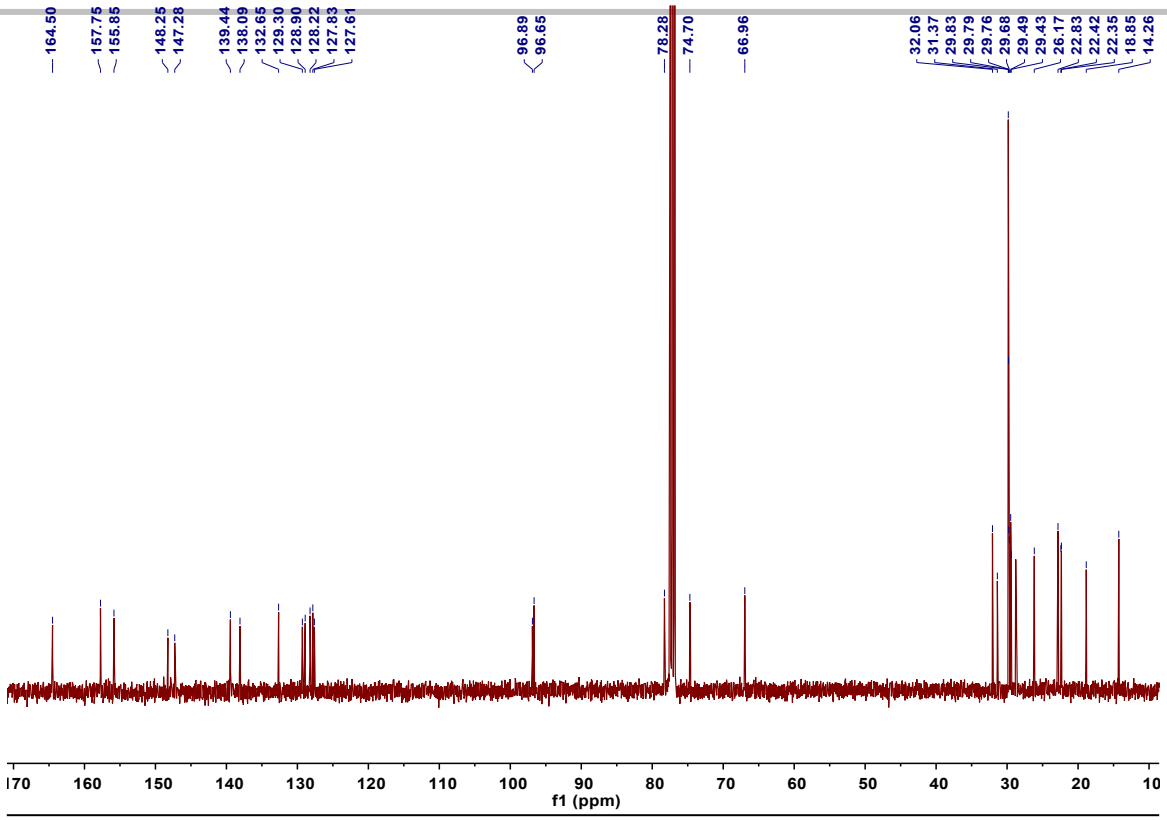

Figure S22. 13C NMR spectrum of complex 3.

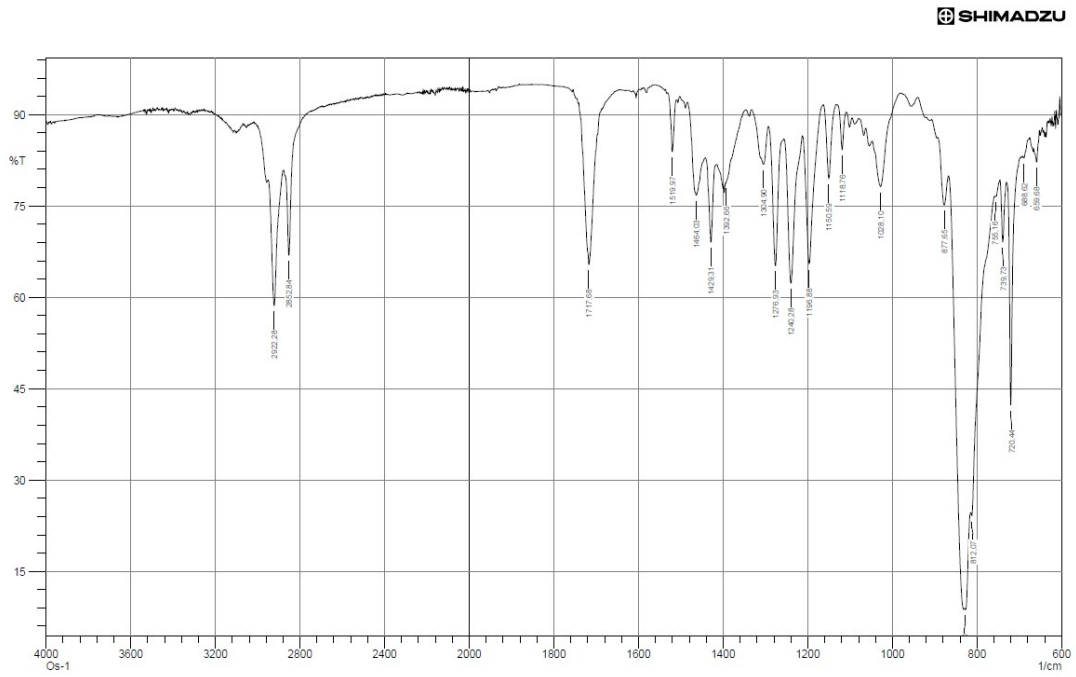

Figure S23. IR spectrum of complex 3.

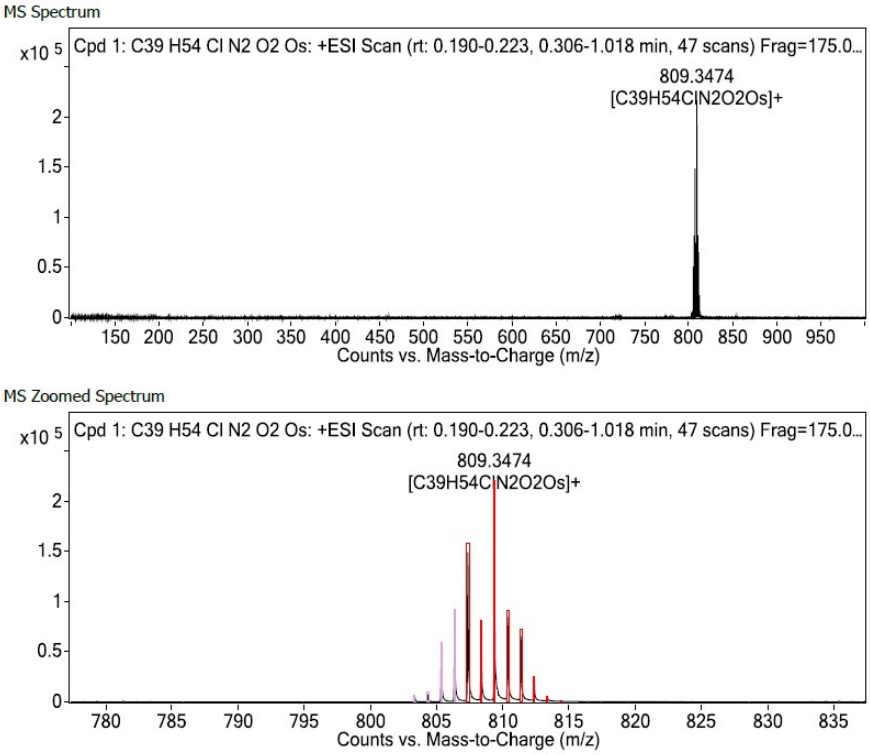

Figure S24. MS spectrum of complex 3.

Synthesis of 4

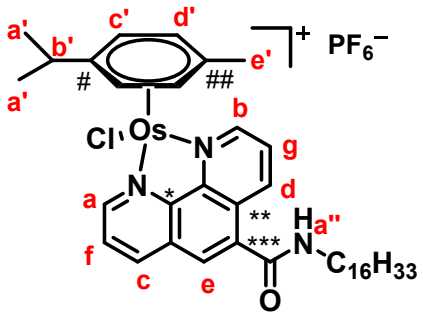

$C_{39}H_{55}ClON_3OsPF_6$
Mr = 952.52 g/mol

A solution of L2 (2 equiv.; 0.03 mmol) and $[Os(\eta^6\text{-}p\text{-cym})Cl_2]_2$ (0.06 mmol) was prepared in 3 mL of $CHCl_3$ and the mixture was refluxed overnight under argon; a solution of NH_4PF_6 (3 equiv; 0.09 mmol) in 1 mL MeOH was then added. A dark yellow solid started to precipitate and the reaction was allowed to run for 2 more hours before discarding the supernatant. A dark yellow residue was obtained, dissolved in CH_2Cl_2, filtered off and evaporated under reduced pressure. The yellow solid was further washed with 10 mL Et_2O, sonicated, filtered and dried under reduced pressure to afford the desired product in 77 % yield.
^{1}H NMR (400 MHz, $CDCl_3$) : δ (ppm) 9.69 (H_a, broad s, 1H), 9.55 (H_b, broad s, 1H), 9.18 (H_c, d, *J* = 9.2 Hz, 1H), 8.65-8.54 (H_{de}, mult, 2H), 7.89-7.83 (H_{fg}, mult, 2H), 7.15 ($H_{a''}$, broad s, 1H), 6.28-6.20 ($H_{c'}$, mult, 2H), 6.02-5.97 ($H_{d'}$, mult, 2H), 3.53 (NH-CH_2-, broad s, 2H), 2.58 ($H_{b'}$, broad s, 1H), 2.22 ($H_{e'}$, s, 3H), 1.69- 1.67 (NH-CH_2-CH_2-, mult, 2H), 1.50-1.24 (-CH_2-, mult, 32H), 0.96 ($H_{a'}$, d, *J* = 4.4 Hz, 6H), 0.87 (-CH_3, t, *J* = 6.8 Hz, 3H). **^{13}C NMR** (101 MHz, $CDCl_3$) : δ (ppm) 165.9 (C=O), 147.7 (C_a), 147.6 (C_b), 134.3 (C_c), 131.4 (C_d), 130.0 (C_e), 129.5 (C_f), 128.1 (C_g), 96.4 ($C^{\#}$), 96.2 ($C^{\#\#}$), 77.3 ($C_{c'}$), 75.6 ($C_{d'}$) 41.4 (-NH-CH_2-), 32.0 (-CH_2-), 31.7 ($C_{b'}$), 30.3 (-CH_2-), 29.8 (-CH_2-), 29.7 (-CH_2-), 29.5 (-CH_2-), 29.4 (-CH_2-), 27.4 (-CH_2-), 23.1 (-CH_2-), 22.9 (-CH_2-), 22.8 ($C_{a'}$), 20.2 ($C_{e'}$), 14.2 (-CH_3). **IR** (cm^{-1}): 2921.3, 2851.9, 1716.7. **ESI-MS** (positive mode) for $OsC_{39}H_{55}N_3OCl$: $[M]^+$, calculated m/z 808.36; found 808.36 $[M]^+$ (2.04 ppm). **HPLC-UV purity:** 96.3 %

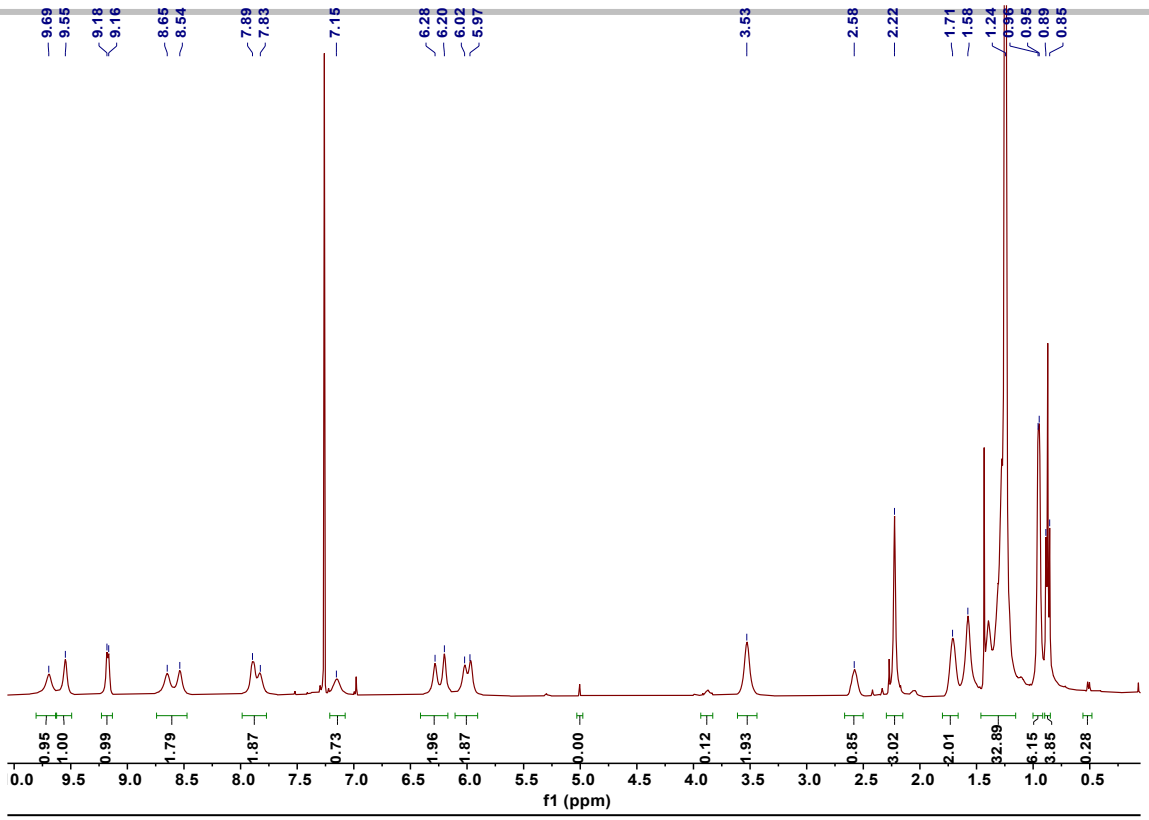

Figure S25. ^{1}H NMR spectrum of complex 4.

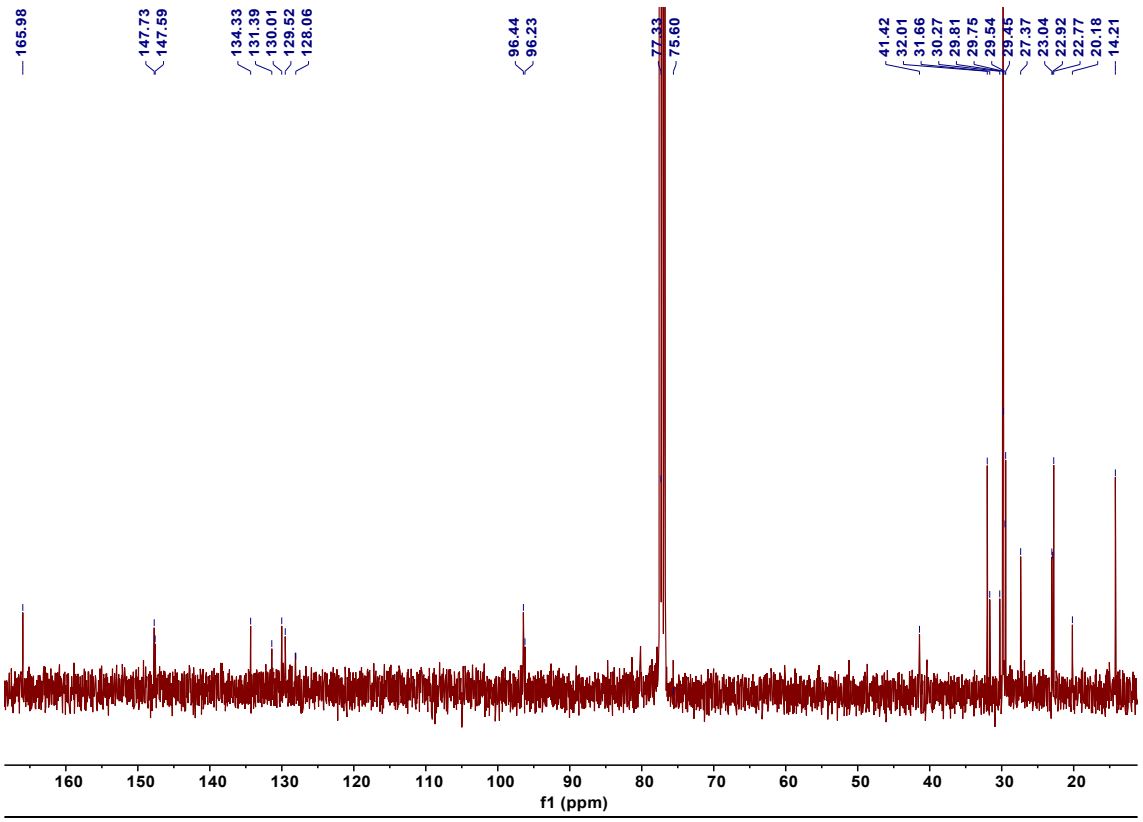

Figure S26. ^{13}C NMR spectrum of complex 4.

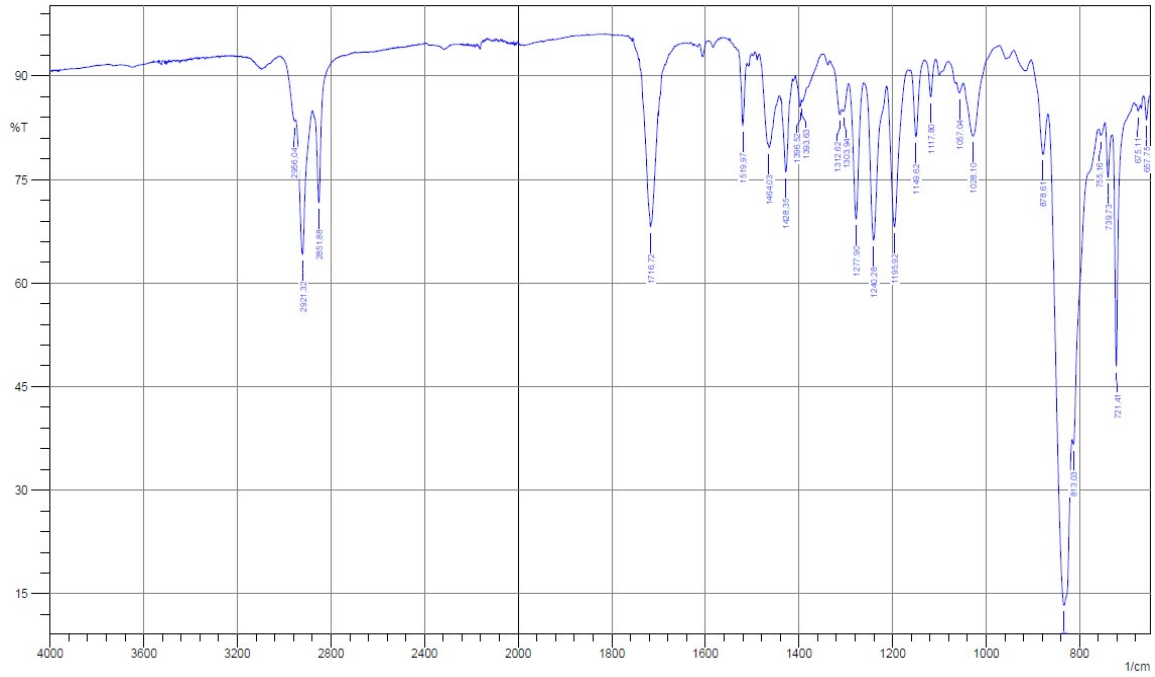

Figure S27. IR spectrum of complex 4.

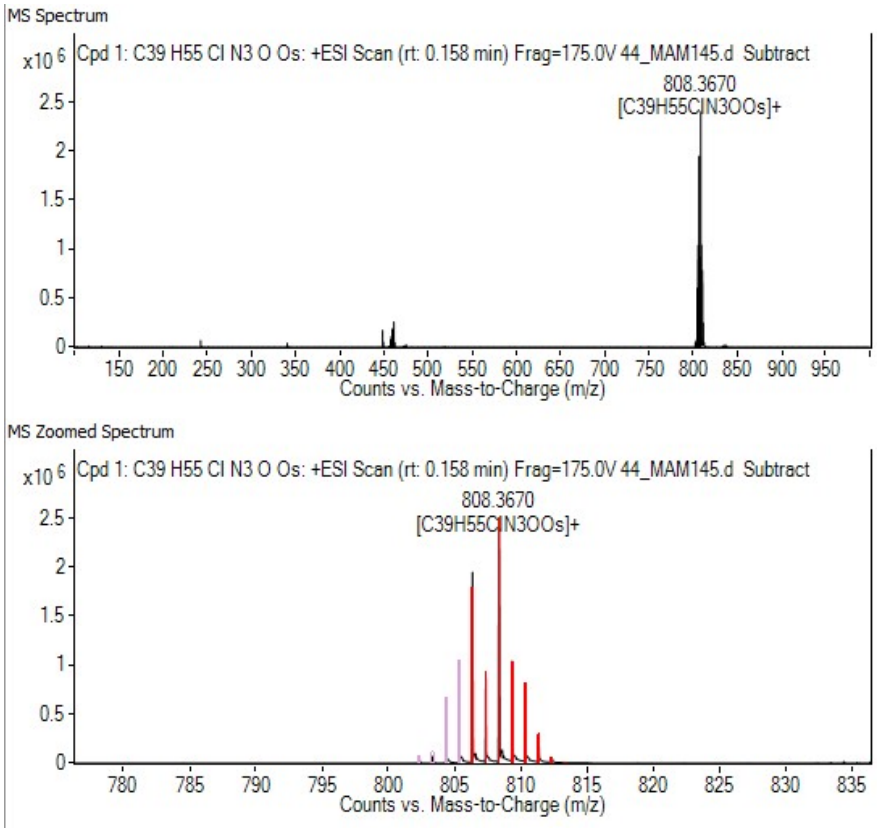

Figure S28. MS spectrum of complex 4.

HPLC-UV

HPLC-UV was performed on an Agilent 1100 series coupled to a binary pump, an UV-Vis diode-array-detector (DAD) detector and a 20 µL sample injector and equipped with a reverse phase ZORBAX Eclipse XDB-C18 column from Agilent. Acetonitrile containing 0.1 % TFA and water containing 0.1 % TFA were used as mobile phases A and B, respectively. Purity was determined by integration of the corresponding UV traces. Solutions of Ru^{II} and Os^{II} complexes at 1 mg/mL were prepared in acetonitrile (5 µL injections). Solvent elution was as follows: 92.5 % solvent A from 0 to 3 min, increasing to 100% at 7 min, 100% from 7 min to 15 min. The data was processed by the Agilent Chemstation software.

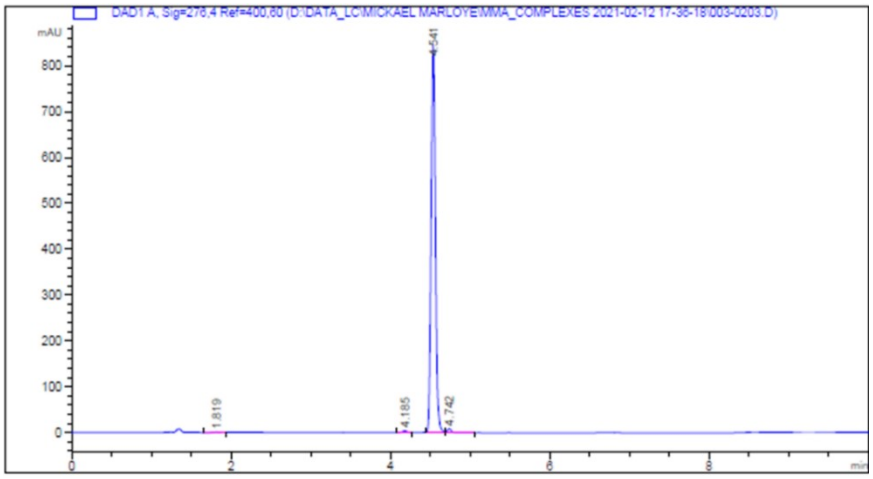

Signal 1: DAD1 A, Sig=276,4 Ref=400,60

Peak #	RetTime [min]	Type	Width [min]	Area [mAU*s]	Height [mAU]	Area %
1	1.819	BB	0.0979	8.29379	1.12634	0.2574
2	4.185	BV	0.0590	15.24853	3.94977	0.4732
3	4.541	VV	0.0597	3166.92480	845.72131	98.2869
4	4.742	VB	0.0530	31.65442	9.01720	0.9824
Totals :				3222.12154	859.81463	

Figure S29. HPLC-UV chromatogram of complex 1.

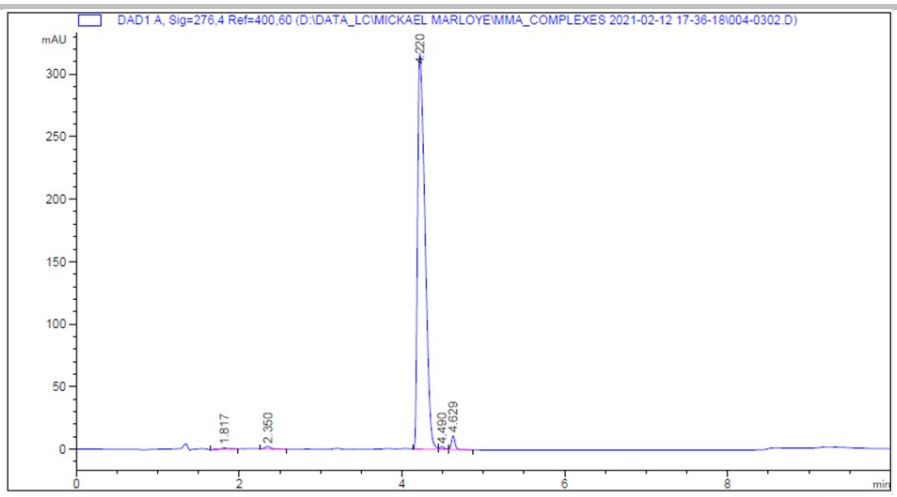

Signal 1: DAD1 A, Sig=276,4 Ref=400,60

Peak #	RetTime [min]	Type	Width [min]	Area [mAU*s]	Height [mAU]	Area %
1	1.817	BB	0.1091	9.72945	1.16948	0.4678
2	2.350	BB	0.0765	10.02655	2.00109	0.4821
3	4.220	BV	0.1043	2016.47803	316.81232	96.9494
4	4.490	VV	0.0602	9.21272	2.22761	0.4429
5	4.629	VB	0.0486	34.48069	11.00297	1.6578
Totals :				2079.92745	333.21347	

Figure S30. HPLC-UV chromatogram of complex 2.

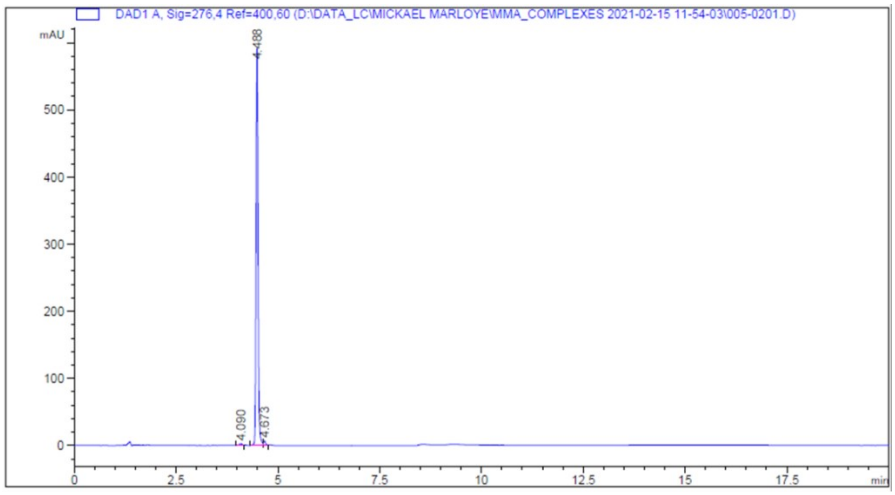

Signal 1: DAD1 A, Sig=276,4 Ref=400,60

Peak #	RetTime [min]	Type	Width [min]	Area [mAU*s]	Height [mAU]	Area %
1	4.090	BV	0.0689	11.93299	2.63268	0.5786
2	4.488	BV	0.0517	2022.76123	593.90796	98.0705
3	4.673	VV	0.0589	27.86389	6.93683	1.3509
Totals :				2062.55810	603.47747	

Figure S31. HPLC-UV chromatogram of complex 3.

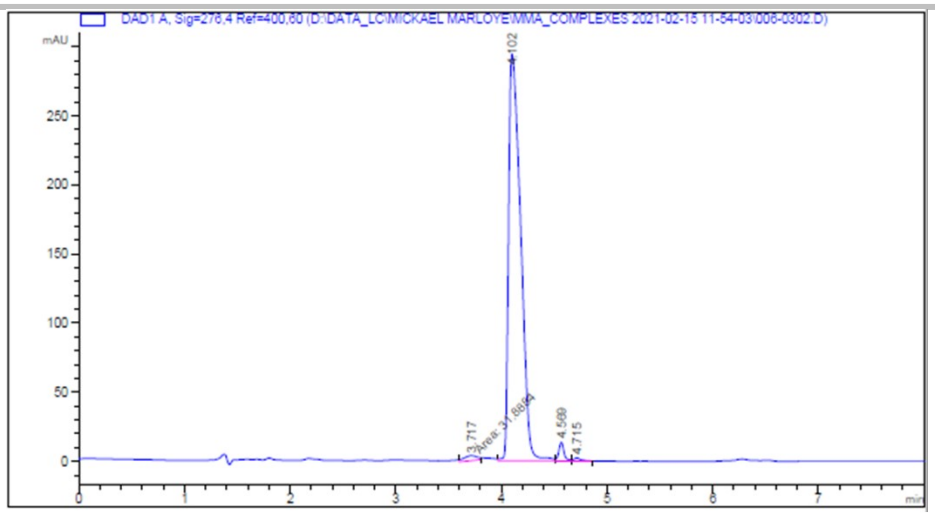

Signal 1: DAD1 A, Sig=276,4 Ref=400,60

Peak #	RetTime [min]	Type	Width [min]	Area [mAU*s]	Height [mAU]	Area %
1	3.717	MM	0.1480	31.88843	3.59047	1.3184
2	4.102	VV	0.1341	2330.01782	294.99600	96.3335
3	4.569	VV	0.0518	46.15928	13.54700	1.9084
4	4.715	VB	0.0700	10.63376	2.13787	0.4396
Totals :				2418.69929	314.27134	

Figure S32. HPLC-UV chromatogram of complex 4.

UV-Vis

UV-Vis spectra were recorded at 25 °C on a Shimadzu UV-1800. Samples were prepared as follows: 1.96 mL H_2O + 40 µL of compounds **1-4** from 5 mM stock solutions in DMSO (final concentration = 10 µM). Data was plotted with OriginPro 8.5.

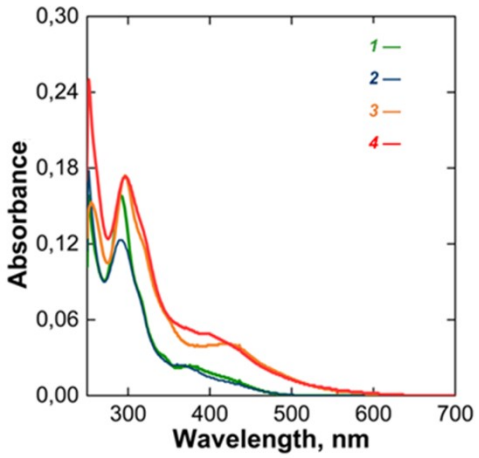

Figure S33. UV-Vis spectra of the four amphiphilic complexes **1-4.**

Structure and solution-state conformation

The correlation map for **2** highlights the close distance between both $H_{a'}$ and $H_{b'}$ from the phenanthroline to H_a, H_b and H_e on the arene. It is stronger for $H_{b'}$, confirming that this hydrogen is at shorter distance to the arene (Figure S2B). Regarding the relative position of the alkyl chain to the phenanthroline ligand (Figure S2C), the amide $H_{a''}$ shows a more intense correlation with $H_{e'}$ than $H_{c'}$, while $H_{b''}$ and $H_{c''}$ better correlate with $H_{c'}$ than H_e'(Figure S2B-C) and in consequence the alkyl chain directly points the opposite direction of $H_{e'}$, as displayed in Figure S2D.

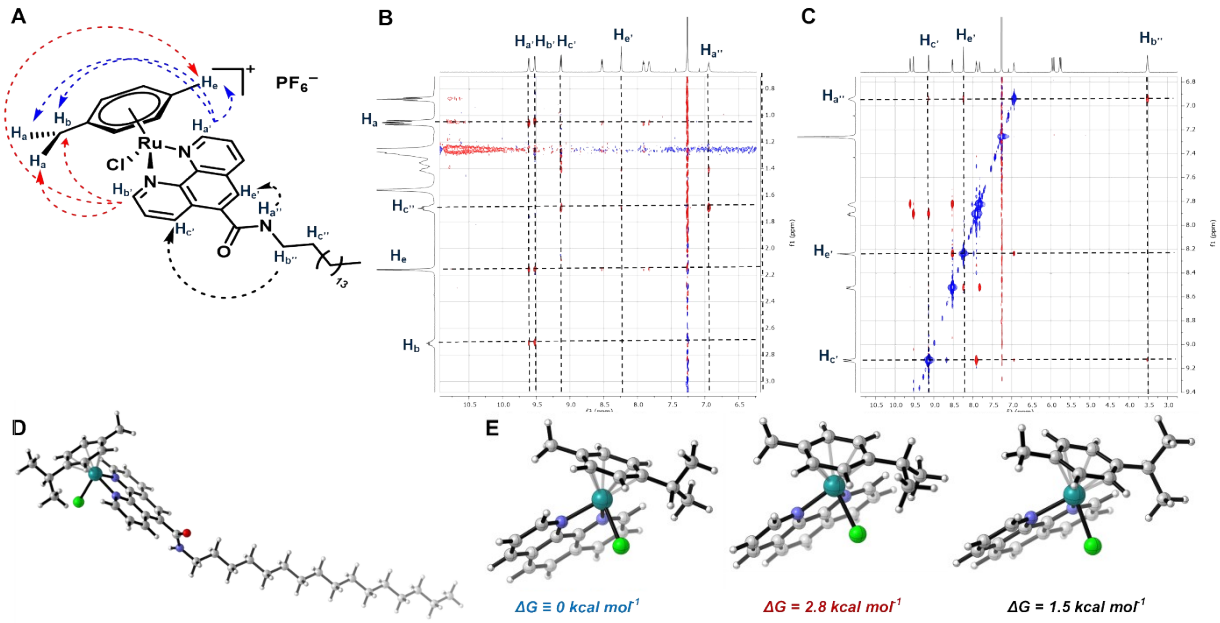

Figure S34. A. 2D-structure of 2 and through-space correlations as determined from ROESY spectra recorded in CDCl3 at 5 mM and 25 °C. B and C. Relevant regions of the ROESY spectra of 2. D. DFT calculated structure of 2 at the ωB97x-D/def2TZVP level of theory. E. Calculated free energies for the arene rotamers (the C16 chain is omitted).

Particle measurement and visualization

Dynamic light scattering

Particle size was first determined on aqueous solutions (PBS – DMSO 1.5 %) at 75 µM. Samples were prepared from 5 mM stock solution in DMSO, under sonication, vortexed for 10 sec and allowed to equilibrate for 2 h before measurements. Particles were then measured by dynamics light scattering (DLS) using a Malvern Zetasizer Nano ZS. Critical aggregation concentrations (CAC) were determined graphically for compounds 1-4 by plotting particle count as a function of the concentration (prepared from successive 4/5 dilution of the starting 75 µM solutions).

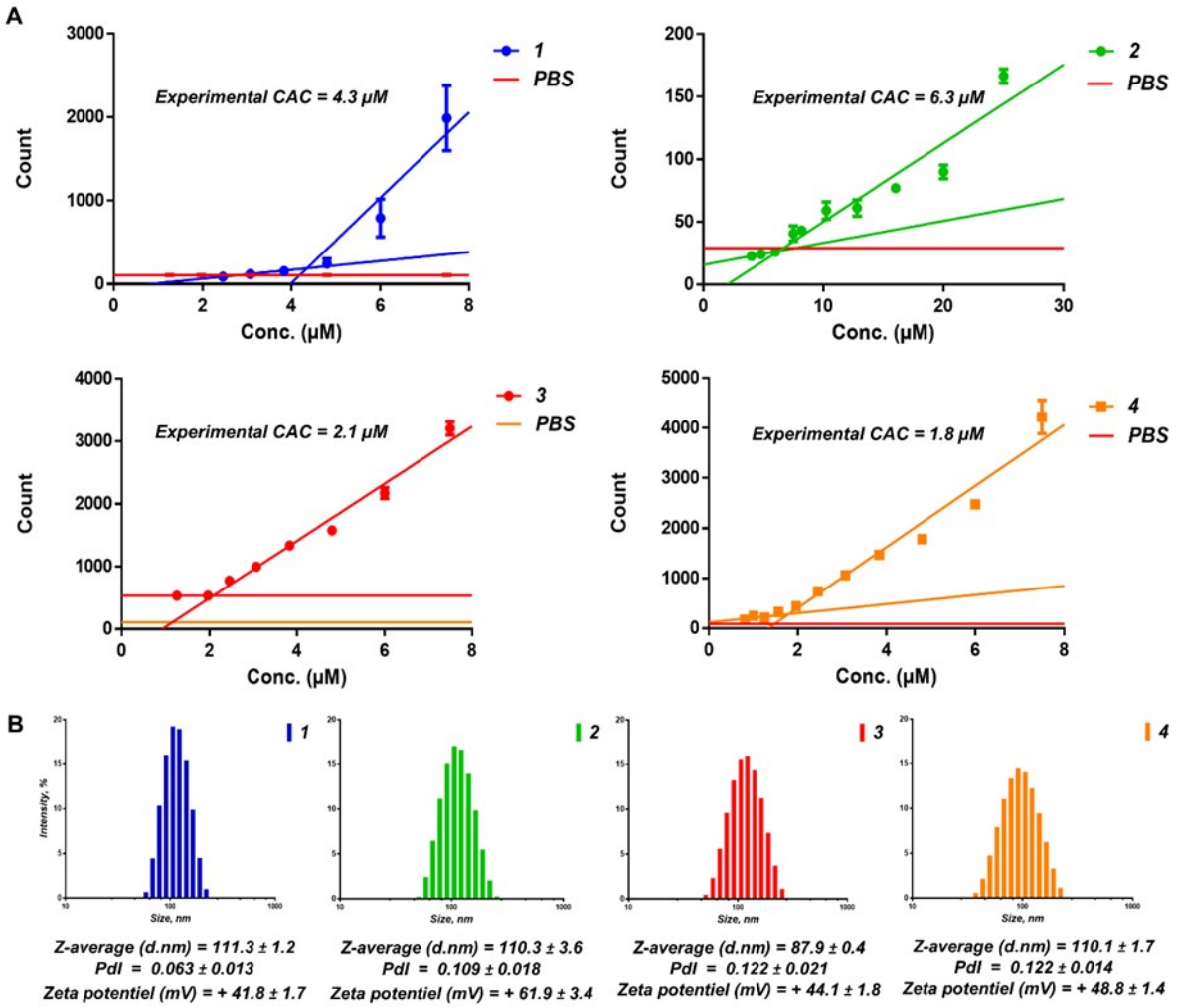

Figure S35. A. Determination of the CAC for amphiphilic compounds **1-4** using plots of particle counts vs concentrations. B. Size distribution, average diameter of the nanoparticles, and zeta potential.

Transmission electron microscopy (TEM)

TEM images of nanoparticles formed by compounds **2** and **4** were obtained from 75 µM solutions (PBS – DMSO 1.5 %). 100 µL of particle suspensions were placed on a carbon-coated EM grid, and 0.4 µL of 25 % glutaraldehyde was added. Particles were then allowed to settle on the grid overnight at 4 °C. Grids were blotted on filter paper and stained for 30 seconds with 2 % uranyl acetate. After further blotting and drying, samples were directly observed on a Tecnai 10 TEM (FEI). Images were captured with a Veleta camera and processed with iTEM.

Reactions with bionucleophiles

Aquation

Reactions were monitored by ^{1}H NMR on a JEOL 600 MHz spectrometer. Aquation of **2** and **4** was performed at 37 °C for 72 h and 18 h in a 7:3 mixture DMSO-d_6/D_2O or 7:3 DMF-d_7/D_2O, respectively, in the presence of 1.5 equiv. of $AgPF_6$. MS samples were prepared in a 7:3 mixture of DMSO/H_2O for 24 h.

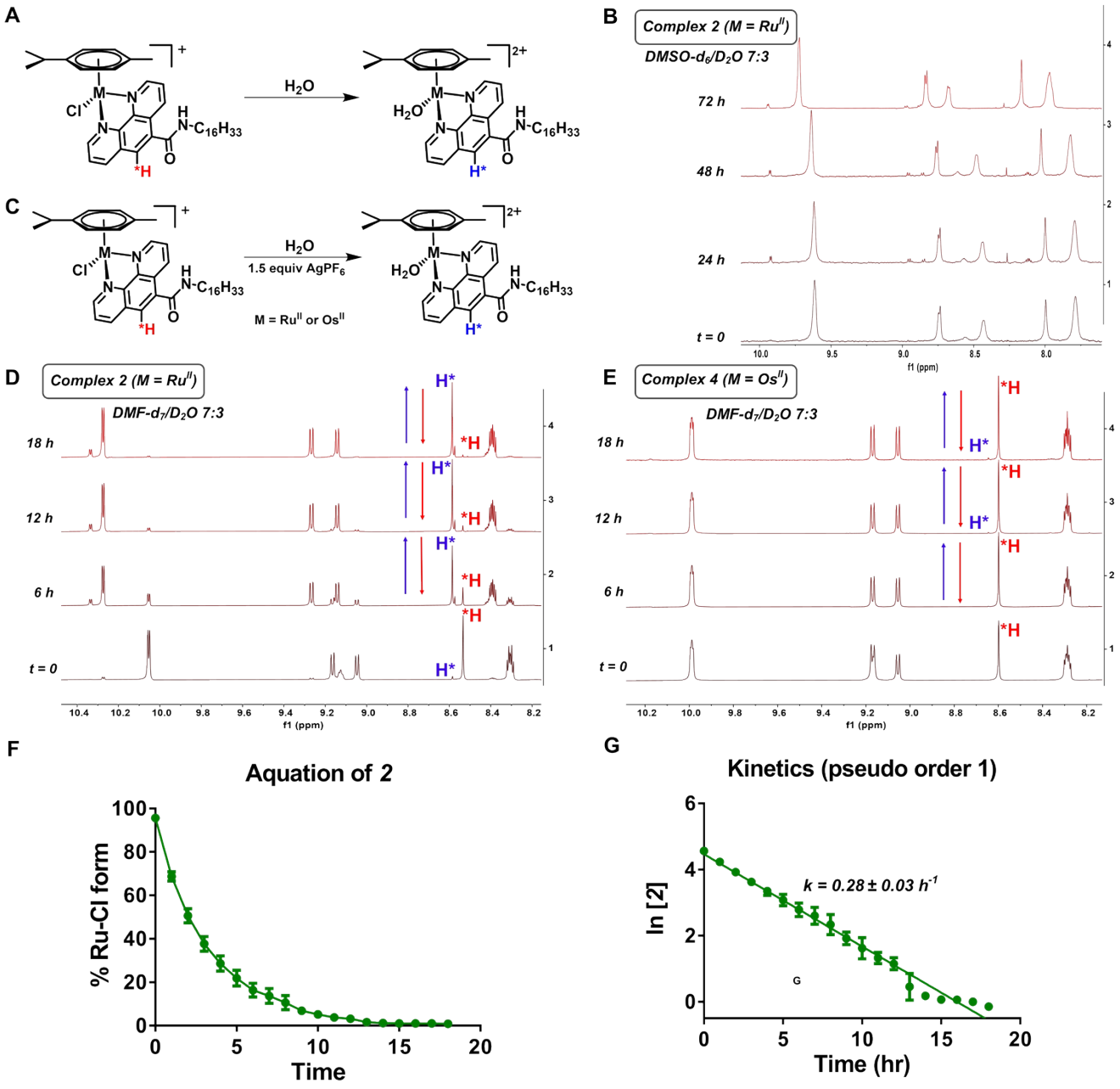

Figure S36. A. Reaction scheme for the aquation reaction of metal complexes **2** and **4**. B. ^{1}H NMR spectral changes during the aquation of **2** (7.5 mM) in DMF-d_7/D_2O (7:3). C. Aquation of metal complexes **2** and **4** with 1.5 equiv. of $AgPF_6$. D and E. ^{1}H NMR spectral changes during the aquation of **2** and **4** (7.5 mM) in DMF-d_7/D_2O (7:3) in the presence of 1.5 equiv. of $AgPF_6$. F. Percentage of compound **2** over time during the aquation process in the presence of 1.5 equiv. of $AgPF_6$. G. Pseudo-first order kinetic plot for the aquation of compound **2** (with 1.5 equiv. of $AgPF_6$).

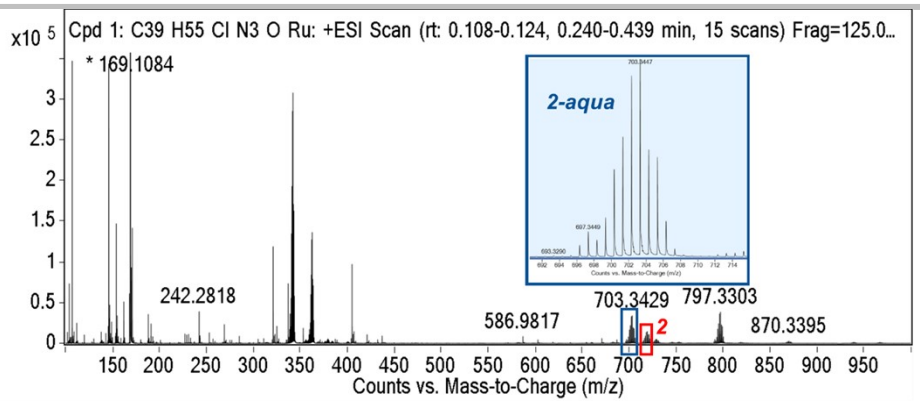

Figure S37. MS evidence for the formation of the aqua complex **2**.

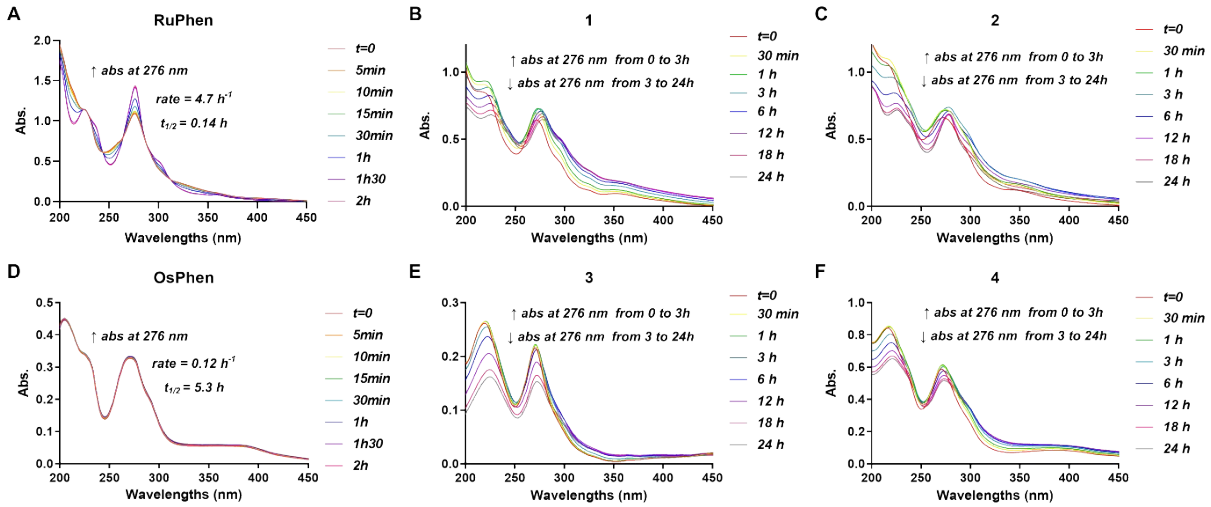

Figure S38. UV-Vis spectra of compounds **1**-**4**, RuPhen and OsPhen. Samples were prepared from stock solutions of the different compounds at 10 mM in acetonitrile and diluted in milliQ water to a final 50 μM concentration (0.5% of acetonitrile). pH was determined for each solution (A) 6.1, (B) 6.0, (C) 5.8, (D) 6.2, (E) 6.4, (F) 6.3.

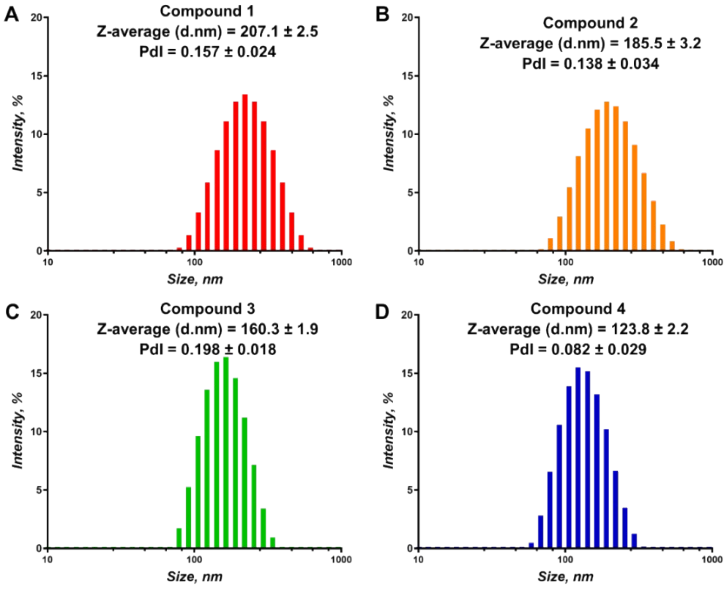

Figure S39. Size distribution and average diameter for nanoparticles obtained from the UV-Vis solutions of compounds **1**-**4**.

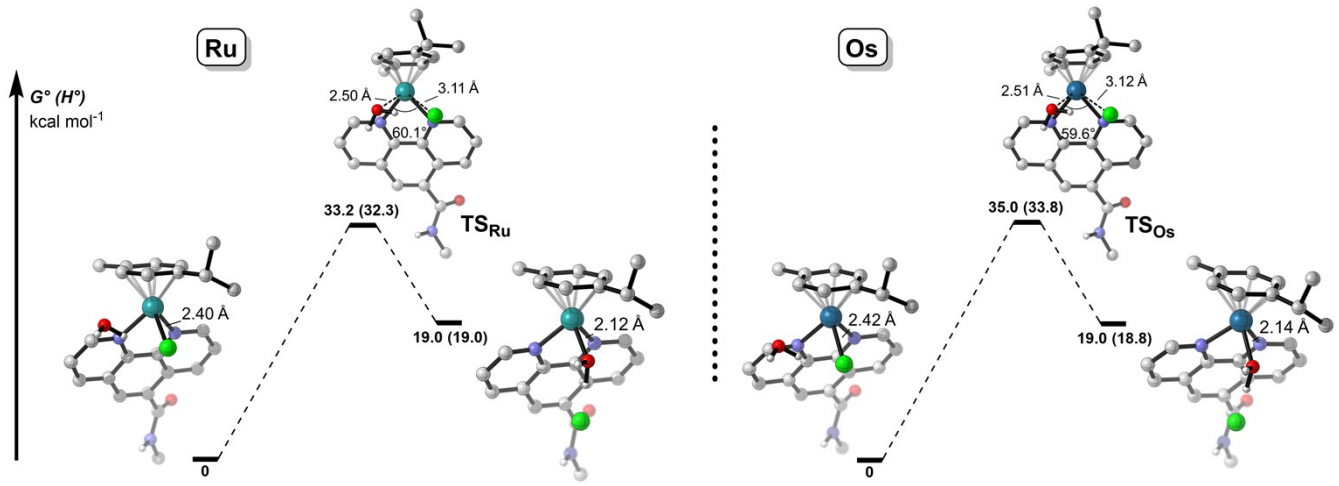

Figure S40. DFT energy profiles at the ωB97xD/def2-TZVP level of theory in water (IEFPCM) for the aquation of truncated **2** (A) and **4** (B). The C16 chain has been replaced by a methyl group.

Glutathione (GSH) and 9-Methylguanine (9-MeG)

Reactions were monitored by 1H NMR on a JEOL 600 MHz spectrometer. Reactions with GSH (1.2 equiv.) for 2 and 4 (at 7.5 mM) were run for 72 h at 37 °C in a 7:3 mixture of DMSO-d6/D2O.

Mass spectrometry was performed on an Agilent Q-TOF-6520 system. m/z from 100 to 1700 were recorded in positive mode. 500 µM solutions of the complexes were reacted with silver (AgPF6, 1.5 equiv) in milliQ water for 24 h at 37°C. The samples were then incubated at 37°C for another 24 h after the addition of GSH (10 equiv.) or 9MeG (10 equiv.). Samples were diluted to 5 µM in a mixture of 0.2% formic acid in water/acetonitrile (2:8) before injection.

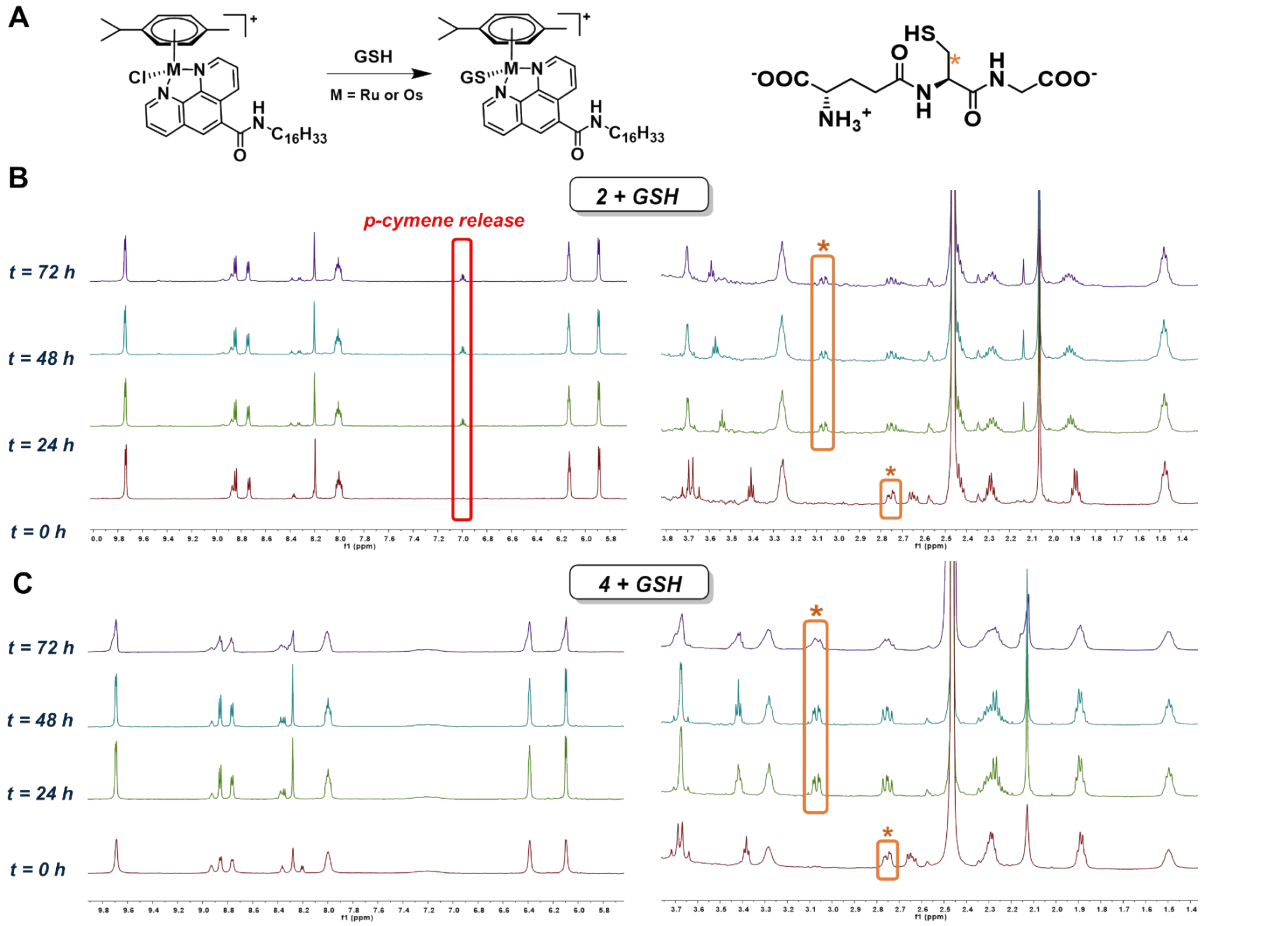

Figure S41. A. Reaction of Ru^{II}/Os^{II} compounds with GSH. B.^{1}H NMR of **2** (7.5 mM) in DMSO-d_6/D_2O (7:3) in the presence of 1.2 equiv. of GSH monitored during 72 h at 37 °C. C. ^{1}H NMR of **4** (7.5 mM) in DMSO-d_6/D_2O (7:3) in the presence of 1.2 equiv. of GSH monitored during 72 h at 37 °C.

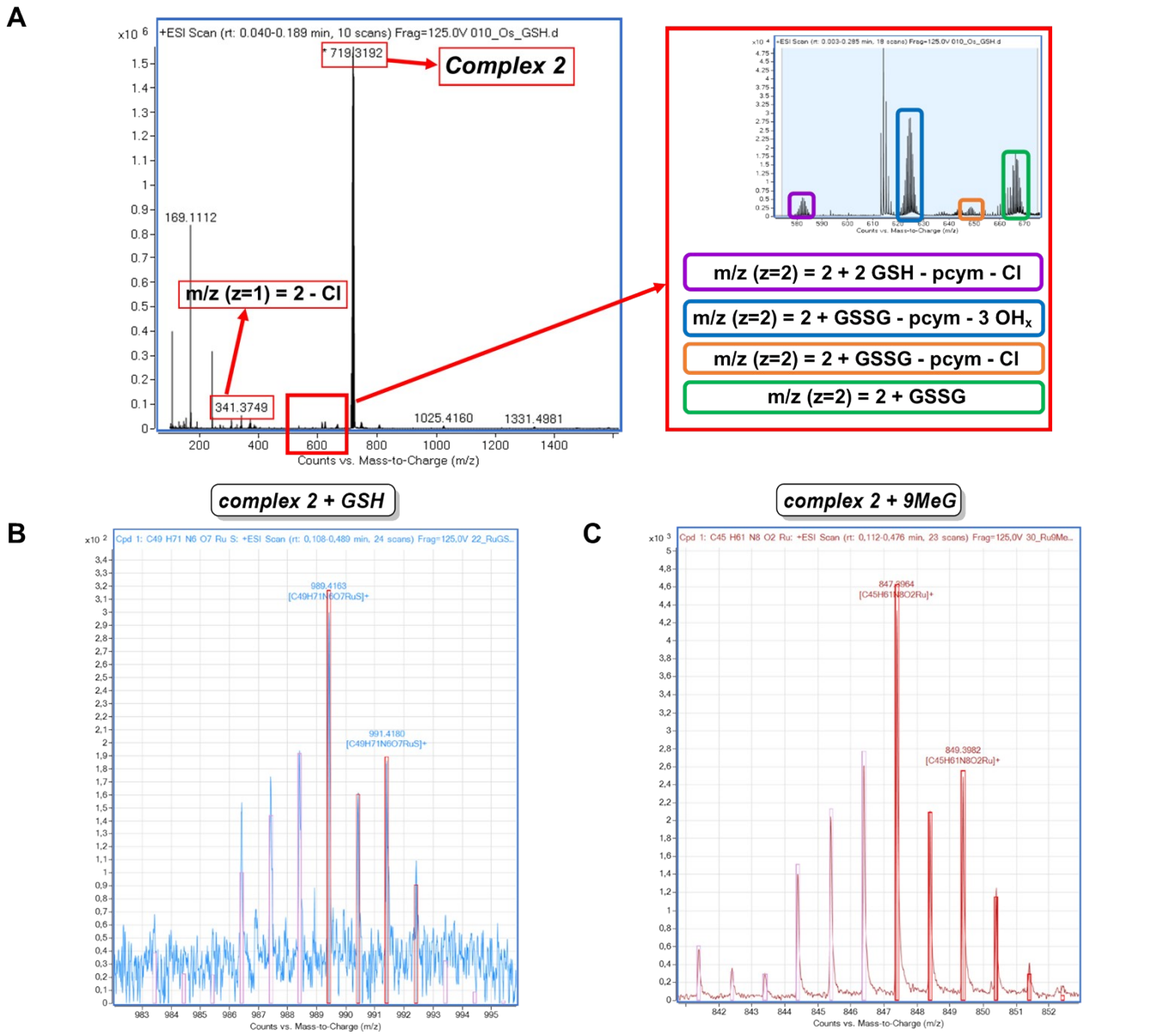

Figure S42. MS spectra of the reaction of **2** with GSH (A and B) or 9-MeG (C), after pre-activation with $AgPF_6$ for 24 h.

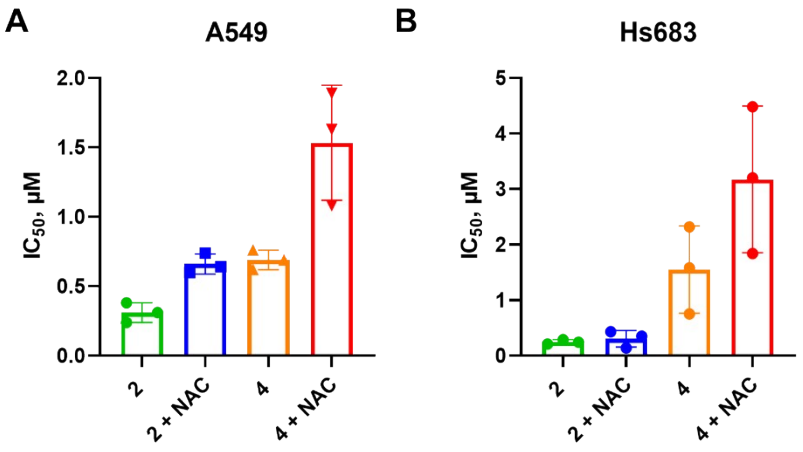

Figure S43. Plots of IC_{50} determined by MTT assays on A549 (A) and Hs683 (B) cell lines for compounds **2** and **4** co-incubated during 72 h with 4 mM N-acetylcysteine. P-values were generated using one-way ANOVA test with GraphPad Prism 6 (*p < 0.05, **p < 0.01, ***p < 0.001).

Binding to Human Serum Albumin

The binding of compounds **1**-**6** to human serum albumin (HSA, A 1653, Sigma-Aldrich, lyophilized, 96-99% by agarose gel, carbohydrate-free and reduced Cys34) was determined by fluorescence spectroscopy. Spectra were recorded on a SpectraMax® iD3 microplate reader between 270 and 600 nm at 25, 30 and 35 °C. Each well contained 200 µL of 2 µM HSA in PBS and 5, 10, 20 and 50 µM of compounds **1-6**. Excitation was set to 297 nm and emission spectra were recorded at λ = 340 nm. The data was fitted to the Stern-Volmer equation (eq 1). Each experiment was conducted once in triplicate.

$$\frac{F_0}{F_0 - F} = \frac{1}{F_a K_a}\frac{1}{Q} + \frac{1}{F_a} \quad \text{(eq.1)}$$

Molecular docking was achieved using Autodock Vina. The protein structure was retrieved from the Protein Databank (human serum albumin complexed with palmitic acid: 1E7H).[6] The starting structure of **2** used for docking was first optimized by DFT. Polar hydrogens were added to the crystal structure 1E7H and the receptor was kept rigid. Rotation in the Ru complex **2** was allowed for single bonds.

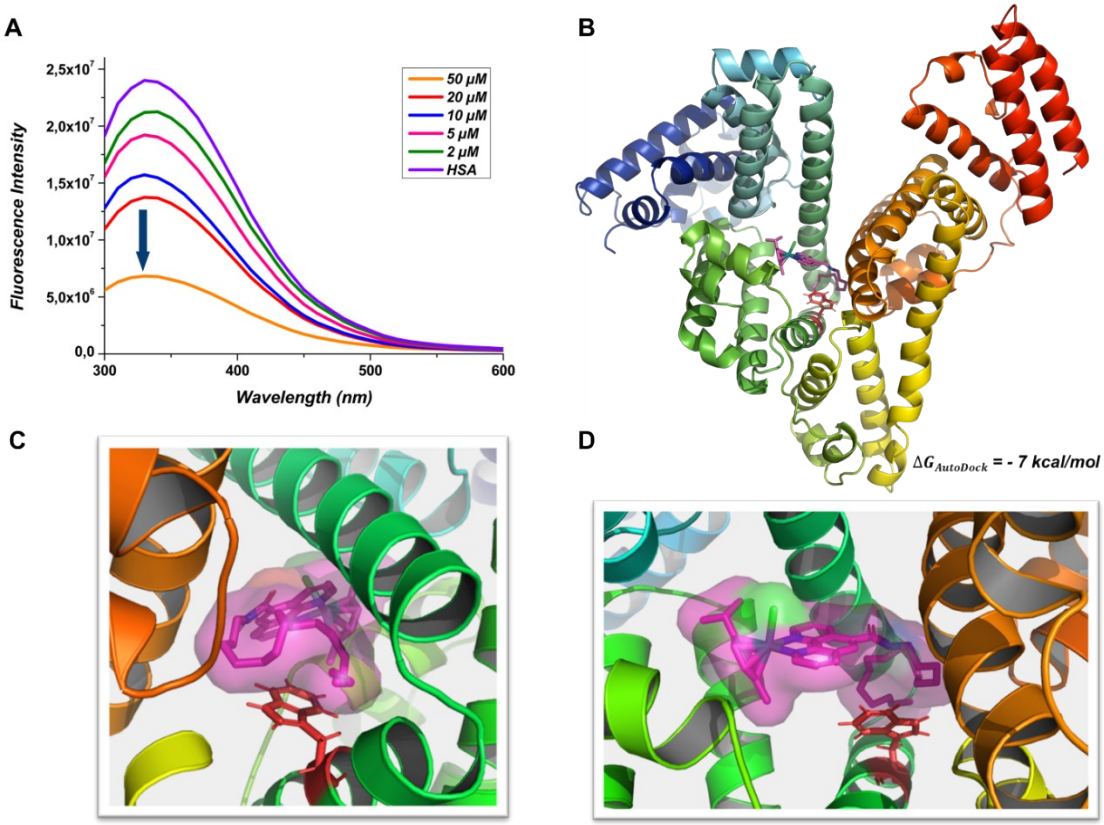

Figure S44. A. Quenching of Trp214 fluorescence by increasing concentrations of **2**. B-D. Molecular docking of the DFT structure of **2** within the HSA binding site IIA (PDB 1HE7).

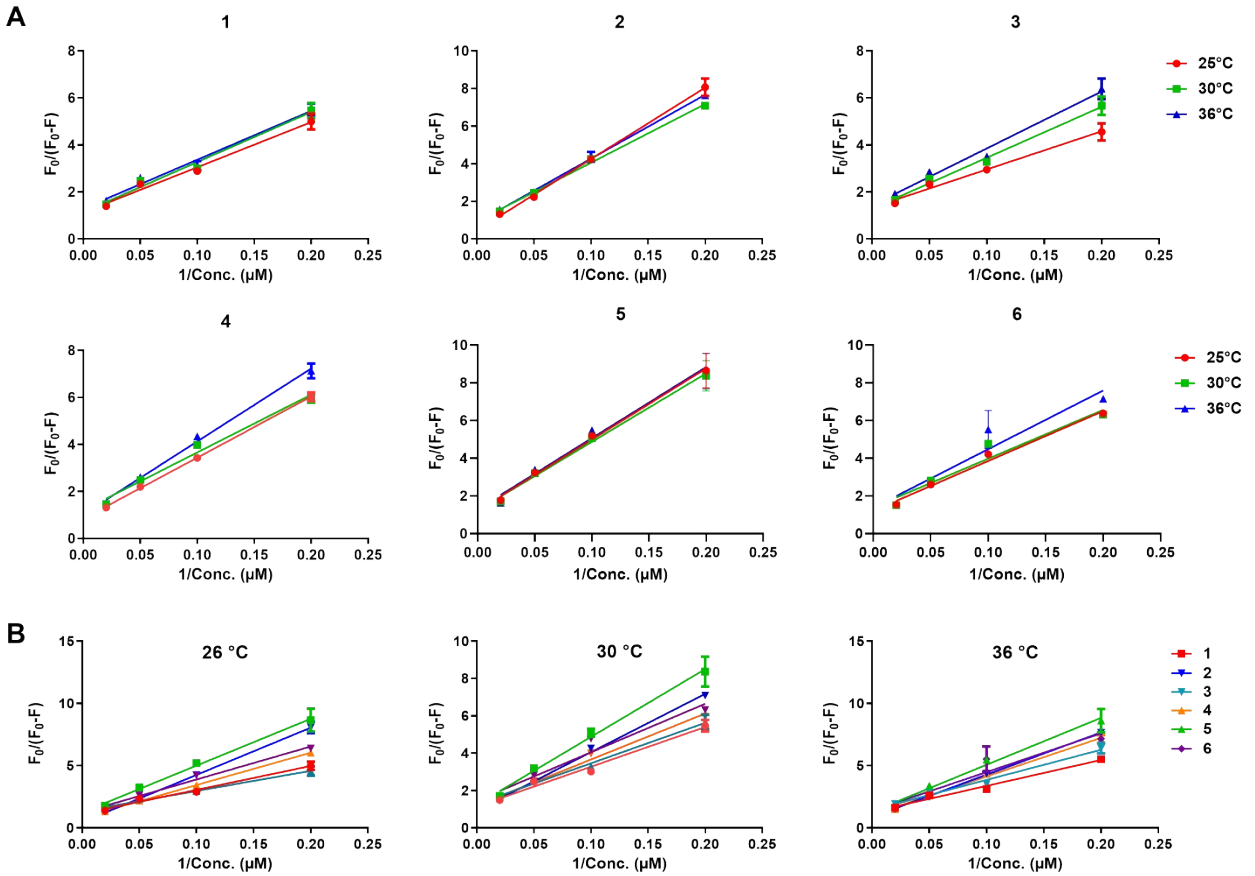

Figure S45. A. Graphical representations of the fluorescence data fitted to the modified Stern-Volmer equation for compounds **1-6** at 5, 10, 20 and 50 μM. B. Graphical representations of the data fitted to the modified Stern-Volmer equation for compounds **1-6** at 5, 10, 20 and 50 μM at 26, 30 and 36 °C.

Table S1. Comparative table of HSA binding affinity for compounds 1-6 (Ka) and derived thermodynamic parameters.

T (*K*)	K_a (10^4 M^{-1})					
	1	**2**	**5**	**3**	**4**	**6**
299	**4.58**	**5.58**	**2.21**	**4.65**	**4.59**	**3.14**
303	**4.12**	**3.46**	**2.28**	**3.60**	**3.39**	**2.81**
309	**3.73**	**3.27**	**2.12**	**2.90**	**3.15**	**2.24**
			ΔG⁰ (kJ/mol)			
299	**-33.3**	**-30.1**	**-15.1**	**-28.2**	**-27.7**	**-21.6**
303	**-32.2**	**-26.6**	**-14.9**	**-24.9**	**-24.6**	**-19.2**
309	**-30.5**	**-21.4**	**-14.6**	**-20.2**	**-19.9**	**-15.7**
			ΔH⁰ (kJ/mol)			
	-116.7	**-289.9**	**-29.6**	**-267.9**	**-256.7**	**-196.7**
			ΔS⁰ (kJ/mol.K)			
	-0.279	**-0.869**	**-0.049**	**-0.801**	**-0.766**	**-0.585**

Quantum mechanical methods

All quantum mechanical calculations have been achieved using Gaussian16 and Orca 4.[7] Geometries of the investigated systems were fully optimized at the spin-unrestricted density functional theory level using the dispersion-corrected ωB97x-D exchange-correlation functional.[8] The balanced polarized triple-zeta basis set def2-TZVP from Ahlrichs and co-workers[9,10] has been used for all atoms, except for the metal, for which either the quasi-relativistic Stuttgart-Dresden core potential was used or, for a better description of relativistic effects for core electrons, an all-electron scalar relativistic approximation (zeroth order regular approximation, ZORA)[11] as implemented in ORCA 4. Potential energy surface minima found upon optimization were confirmed by frequency calculations and free energies were corrected to account for the zero-point energy. Optimized geometries were verified as minima (*i.e.* zero imaginary frequencies). The Synchronous Transit-Guided Quasi-Newton method[12,13] was used for locating transition structures. These structures were further verified as saddle points by frequency calculations (*i.e.* one and only one imaginary frequency). The bulk solvent effects have been included through the Integral Equation Formalism version of the Polarizable Continuum Model.[14]

Biological assays

MTT assays

First-line evaluation of the growth inhibitory potency of all compounds used the colorimetric MTT (3-[4,5-dimethylthiazol-2yl]-2,5-diphenyltetrazolium bromide, Sigma) assay. The human glioma Hs683 (ATCC, code HTB-138), human non-small cell lung cancer A549 (DSMZ, code ACC107), human breast adenocarcinoma MCF7 (ATCC, code HTB-22), murine lung carcinoma M109 (ATCC, code TCP-1016) and the murine metastatic melanoma B16F10 (ATCC, code CRL-6475) cell lines were used. All the cell lines were maintained under a controlled atmosphere (37 °C, 5 % CO_2) in RPMI1640 supplemented with heat-inactivated (56 °C, 1 h) fetal bovine serum (10%), glutamine (2%), penicillin-streptomycin (2%) and gentamicin (0.2%); all of these reagents were purchased from Lonza. The cells were seeded in 96-microwell plates (the seeding density varied between 800 and 1200 cells in 100 µL of medium per well, depending on the cell line) 24 h before treatment to ensure adequate cell adhesion. The anticancer compounds were then assayed from 5 to 50 µM for 72 h (from 5 mM stock solutions in DMSO); final concentration of DMSO is thus 1% for the highest compound concentration (50 µM). Control cells were treated with the highest concentration of DMSO (1%) and no difference in term of viability was observed between cells treated with 1% DMSO and untreated cells. The cell population growth in the control and treated samples were determined according to the capability of living cells to reduce the MTT yellow product (0.5 mg/mL in white RPMI1640 medium; 100 µL/well) during a minimum of 3 h into formazan blue crystals. After centrifugation at 200 g for 8 min and removing of the MTT solution, the crystals were solubilized in DMSO (100 µL/well). Plates were read on a Biorad Model 680XR at 570 nm. Each experiment was repeated three times independently.

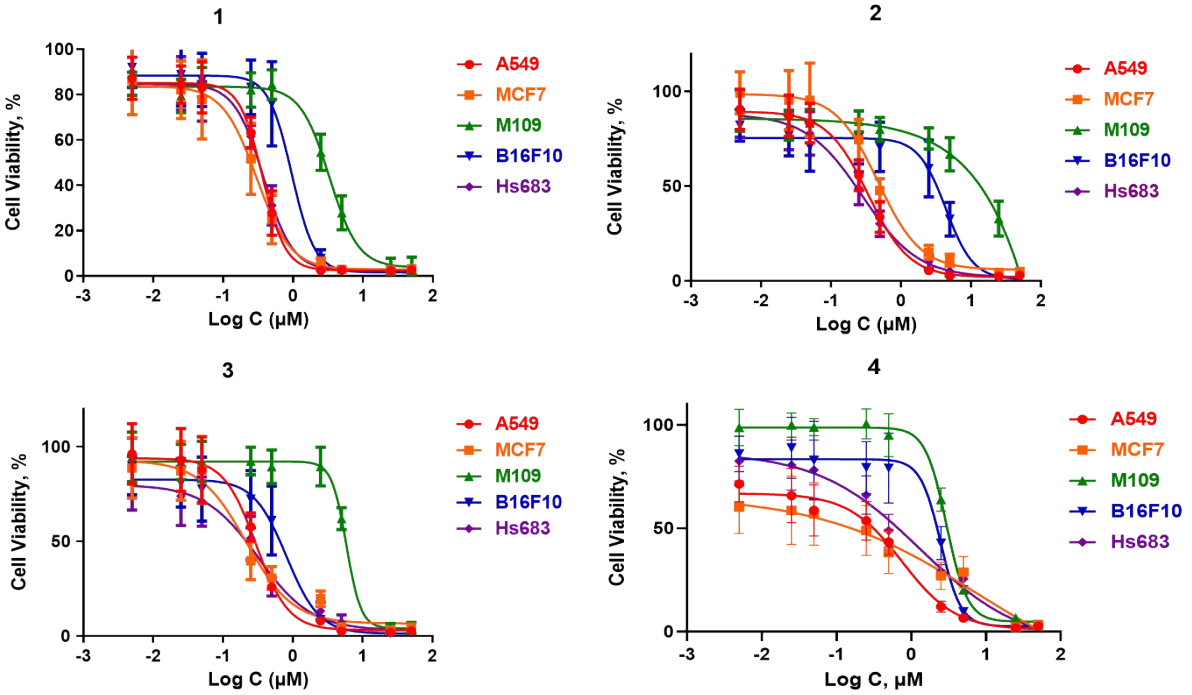

Figure S46. Experimental cytotoxicity curves obtained from MTT assays for compounds **1**-**4**.

Cellular accumulation by ICP-MS

Approximately 1x10^6 cells were seeded in T25 flasks and incubated for 24 h. Cells were then treated with the cytotoxic agent at 2 µM and incubated for 16 h at 37 °C in a 5% CO_2 atmosphere. Culture medium was removed, the cells washed with PBS (3 x 1 mL), harvested by trypsinization (1 mL) and neutralized with RPMI medium. Cell-containing suspensions were centrifuged at 1200 rpm for 5 min (25 °C) and the cell pellets were washed three times with 3 mL PBS, before being resuspended in 100 µL of 70% HNO_3 and digested at 60 °C for 1 h. 400 µL of a metal-stabilizing aqueous solution (acetic acid 0.05 % v/v, thiourea 0.01 M and ascorbic acid 0.1 g/L) were then added to the Os samples to avoid the release of the volatile and toxic OsO_4 that may form under oxidative conditions.[15] Metal contents in all samples were determined by inductively coupled plasma mass spectrometry (ICP-MS) on an Agilent 7700 system, where indium (In) was used as internal standard for correcting the instrumental drift. Each experiment was performed in triplicate.

Video-microscopy analysis

Video-microscopy experiments were conducted to observe the morphological changes induced by treatment with complexes **1**-**6**. A549 cells were seeded in T25 flasks (Sarstedt AG & CO) and allowed to attach and start growing for 24 h. Cells were either left untreated or treated with compounds **1**-**6** at their IC_{50}. Pictures of living cells were taken every 4 min during 72 h with 40x optical magnification (Leica). Each experiment was conducted in triplicate. Growth inhibition, duration of mitosis, average number of mitosis and migration characteristics (maximum relative distance from the origin, MRDO) over 72 h were extracted from video-microscopy images by means of an algorithmic method based on the mean-shift principles and the use of adaptive combinations of linked kernels.[16] This approach allows the detection of various gray-level configurations and the transition between them.

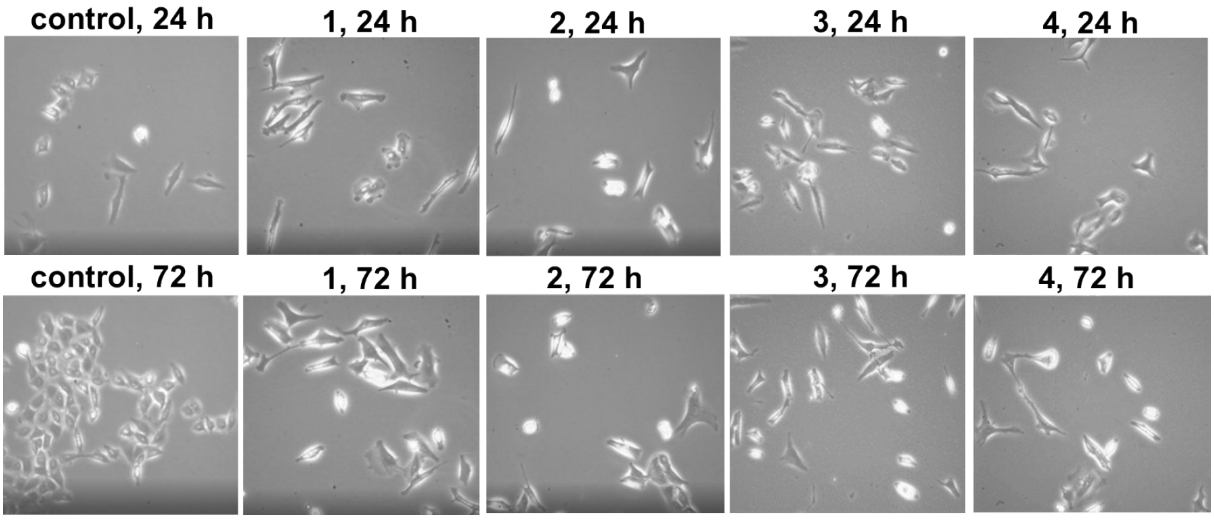

Figure S47. Video microscopy experiment snapshots on the A549 cell line following treatment with the amphiphilic compounds 1-4 at their IC_{50}.

Growth inhibition, mitotic events, and motility parameters were then quantified over the 72h time lapse (Figure S48). Growth inhibition for compounds **1**-**6** confirmed the results obtained from MTT assays (Figure S48A). Mitotic events closely reflected the potent antiproliferative activity of amphiphilic compounds **1**-**4** compared to the non-amphiphilic compounds **5**-**6** and the control, showing a strong reduction in mitotic activity (Figure S48B), although no significant changes were observed between compounds **1**-**6** and controls in terms of mitosis duration (Figure S48C). The maximum relative distance from the origin (MRDO) was used to determine cell motility. The Ru^{II} ester **1** seemed to slightly promote migration in comparison to other metal compounds for which a decrease in migration was observed in comparison to control (Figure S48D).

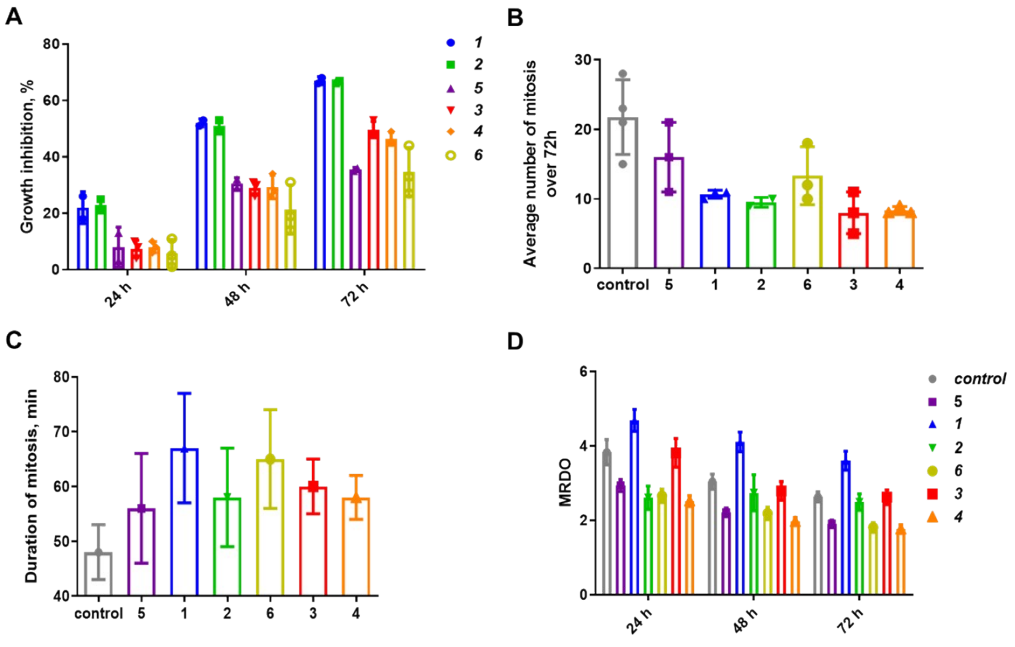

Figure S48. Data were obtained from videomicroscopy experiments. A. Growth inhibition as calculated from the videomicroscopy. B. Average number of mitosis over 72 h. C. Duration of mitosis. D. MRDO (maximum relative distance from the origin) was obtained over 72 h and used to determine migration characteristics.

Measured Log P

The lipophilicity of the compounds was determined experimentally by measurement of the water-octanol partition coefficient (Log P). In this case PBS was used instead of water and octanol was pre-saturated with PBS overnight. Each complex (**1**-**6**) was tested at 50 µM in a mixture of equal volume of PBS and octanol (300 µL) with continuous shaking at room temperature for 3 h in triplicate. The two phases were separated after centrifugation and the metal content (Ru or Os) in each phase was determined by ICP-MS (Agilent 7700) where indium (In) was used as internal standard for correcting the instrumental drift. Each experiment was performed in triplicate.

Apoptosis

We used the Annexin V-FITC/PI detection kit from BD Biosciences (#556547). A549 cells were seeded in 60 mm x 10 mm T25 cm^2 flasks for 24 h before the treatments with or without compounds **1-4**, cisplatin as positive control and no treatment for negative control; these were added to the cells at three different time intervals *i.e.* 15 h, 24 h and 48 h at their IC_{50} concentrations. Briefly, cells were washed twice with cold PBS and then resuspended in binding buffer at a concentration of $1x10^6$ cells/mL. 100 µL of the cell suspension ($1x10^5$ cells) is added to a 5 mL culture tube, annexin V-FITC and PI were then added and incubated for 15 min at RT in the dark. 400 µL of the binding buffer was added before flow cytometry analysis using a Gallios cytometer (Beckman Coulter, Analis). $1x10^4$ events per sample were recorded and each experiment was conducted once in triplicate. Data was analyzed with FlowJo 10.7 and GraphPad Prism 6.0.

Cell cycle analysis

A549 cells were seeded in 6-well plates for 24 h before treatments with **1**-**4** at their IC_{50} concentrations as determined by MTT (see Table 1). The cell cycle was then analyzed with propidium iodide staining (PI, Sigma Aldrich, P4170) in presence of RNAse (Roche 10-109-169-001). Briefly, cells were detached by trypsin and centrifugated (1200 rpm at 4 °C), the supernatant was removed and the cells were resuspended in PBS (2 mL). These operations were repeated twice, before resuspension in ice-cold ethanol (70%) and overnight storage at -20 °C for permeabilization. The cells were then centrifugated (5 min, 1200 rpm) and washed twice with 3 mL PBS and resuspended in a solution of 80 µmg/mL propidium iodide containing RNAse A (0.2 mg/mL). The samples were finally analyzed by flow cytometry on a Gallios cytometer (Beckman Coulter, Analis). $1x10^4$ events per sample were recorded and each experiment was conducted once in triplicate. The flow data was analyzed with FlowJo 10.7.

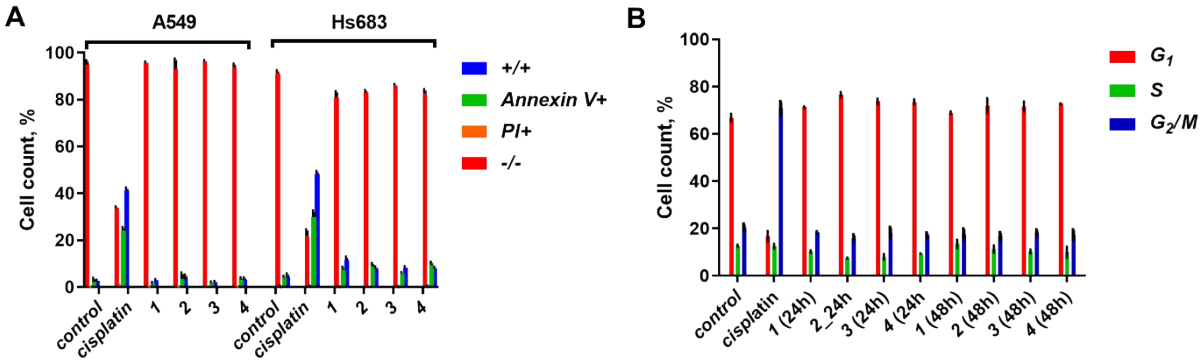

Figure S49. A. Annexin V/PI assays on A549 and Hs683 cell lines for compounds 1-4 at their IC_{50}, after 72 h treatment. B. Propidium iodide and RNAse A staining for cell cycle on A549 cell line following treatment at 15, 24 and 48 h for compounds 1-4, with cisplatin as positive control.

ROS contents

Hs683 and A549 cell lines were seeded in T25 flasks 24 h before treatment with compounds **1-4** at their IC_{50} concentrations for 15 h, 24 h and 48 h (4 mM of H_2O_2 during 2 h was used as positive control). Reactive oxygen species (ROS) were quantified with the fluorescent probe 2′,7′-dichlorofluorescin diacetate (DCFH-DA). DCFH-DA was added to each flask to obtain a final concentration of 20 µM and the flasks were then incubated for 1 h at 37 °C. Cells were washed twice with PBS, detached by trypsin and pooled with their own supernatant that could contain late apoptotic and detached cells. Cells were centrifugated for 5 min at 600 rpm at 4°C and washed twice with PBS. After the last centrifugation, the supernatant was discarded and pellets were finally resuspended in 1 mL cold RMPI without red phenol. Fluorescence measurements were undertaken with a Gallios cytometer (Beckman Coulter, Analis).

1x10^4 events per sample were recorded and experiments were performed in quadruplicate. Data were analyzed with FlowJo 10.7. P-values were generated using one-way ANOVA test with GraphPad Prism 6.0. (*p < 0.05, **p < 0.01, ***p < 0.001).

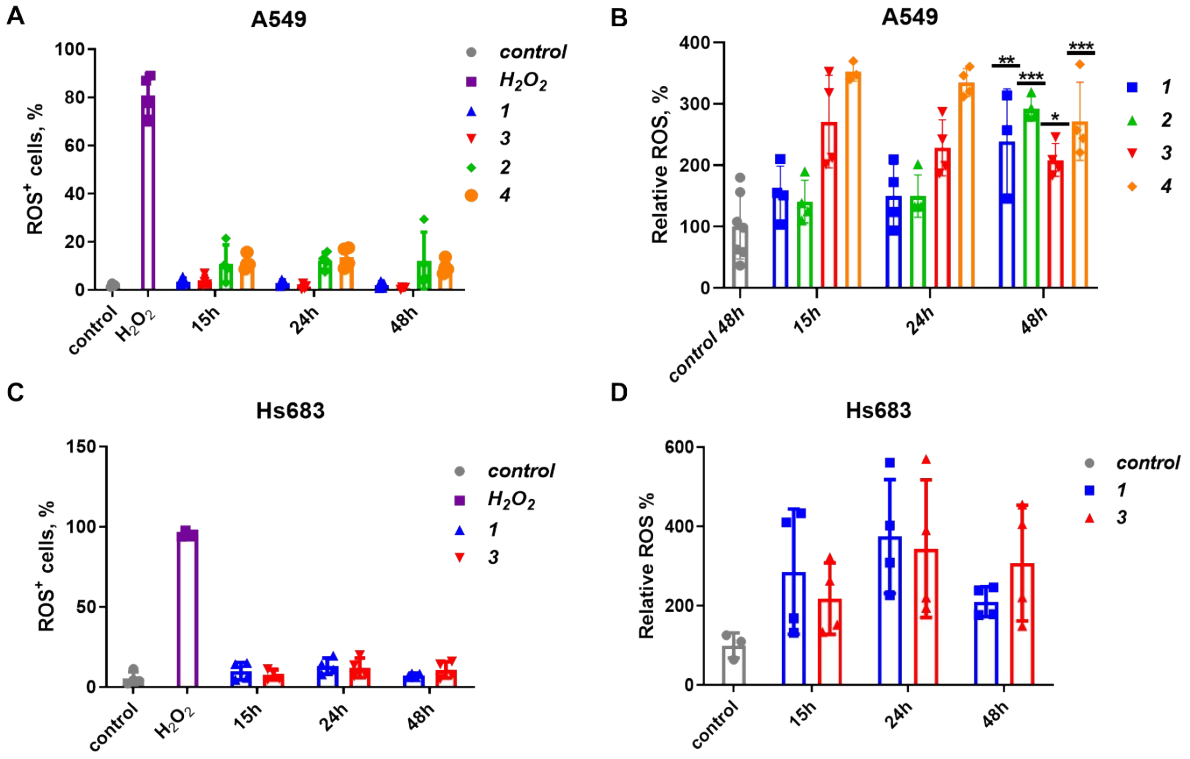

Figure S50. A. ROS contents on A549 cells following treatment for 15 h, 24 h and 48 h with compounds **1-4**, H_2O_2 is used as positive control. B. Relative ROS contents on A549 cells following treatment at 15h, 24h and 48h for compounds **1**-4. C. ROS contents on Hs683 cells following treatment at 15 h, 24 h and 48 h for compounds **1** and **3**, with H_2O_2 as positive control. D. Relative ROS contents on Hs683 cells following treatment at 15h, 24h and 48h for compounds **1** and **3**. P-values of 48 h treatment were compared to the control and were generated using one-way ANOVA test with GraphPad Prism 6 (*p < 0.05, **p < 0.01, ***p < 0.001).

γH2AX and LC-3b

1x10^6 (γH2AX) and 2x10^5 (LC-3b) G9-pCDH cells were seeded in triplicate and treated with the indicated therapies. After 24 h, cells harvested, washed with PBS, fixed with 4% formaldehyde for 20 minutes at room temperature, permeabilized with permeabilization medium (Medium B, #GAS002S5, Thermo Fisher Scientific) and stained with anti-γH2AX(Ser139) (clone 2F3, AlexaFluor 647 Biolegend) or anti-LC3B (clone 1251A, AlexaFluor 647, R&D Systems) for 40 minutes at room temperature. Flow cytometry was performed using a BD Fortessa or BD Aria flow cytometer, 1x10^4 events per sample were counted. Data were analyzed with FlowJo 10.7 and GraphPad Prism 6.0.

Acridine orange

A549 cell lines were seeded in 60 mm x 10 mm 6-well plates (with a microscopy coverslip) for 24 h and 48 h before treatment with compounds **1-4**, cisplatin as positive control and no treatment for negative control; these were added to the cells at two different times, 24 h and 48 h, at their IC_{50} concentrations. After 24 h and 48 h, cells were treated with 1 µg/mL acridine orange (Sigma-Aldrich) as final concentration in the culture medium for 15 min at 37 °C. Cells were washed twice with PBS and kept in RPMI without phenol red before analysis. Coverslips were taken off the 6 well plates, rinsed with PBS and placed on a microscope slide. Each slide was analyzed with an Imager M2 fluorescence microscope (Carl Zeiss) coupled with the AxioCam ICm1 and AxioImager software (Carl Zeiss). Each experiment was conducted once in triplicate.

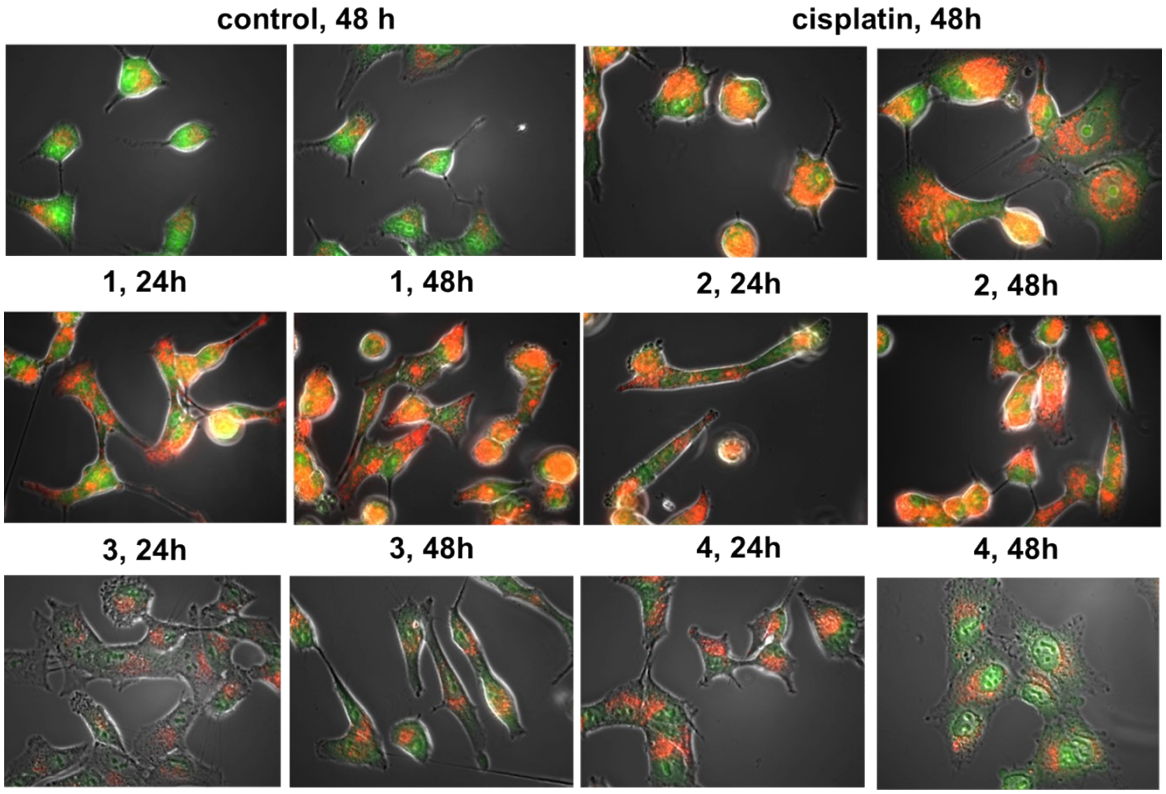

Figure S51. Microscopy images of A549 cells stained with acridine orange and treated with compounds 1-4 at their IC_{50} for 24 and 48 h.

Organelles analysis by TEM microscopy

A549 cell lines were seeded in T25 flasks 48 h before the treatments with **2** and **4** at their IC_{50}, and no treatment for the control. Cells were fixed with 2.5% Glutaraldehyde (EMS), 2% PFA in 0.15 M cacodylate buffer (pH 7.4, Sigma) for 30 min at room temperature and washed in 0.15 M cacodylate buffer (pH 7.4) 5X3 minutes. For the post-fixation step, cells were suspended in 1% osmium tetroxide (EMS) and 1.5% ferrocyanide (EMS) in 0.15 M cacodylate buffer for 1 h at RT and the washed with ultrapure water (UPW) 5X3 min. Solution was changed for 1% osmium tetroxide in 0.15 M cacodylate buffer for another hour at room temperature and cells were washed cells with ultrapure water UPW 5X3 min. Cells were stained with 1% uranyl acetate (EMS) for 1 h at room temperature, washed cells in UPW 5X3 min, and dehydrated in alcohol series 50 %-70 %-90 %-100 %-100 %-100 % for 5 min each. Samples were directly observed on a Tecnai 10 TEM (FEI). Images were captured with a Veleta camera and processed with iTEM.

Mito-stress Test using Seahorse XFe96

A549 cells were seeded at a density of 2 x 10^4 cells/well in a 96 well Seahorse XFe plate the night before the assay and allowed to adhere. The compounds were dissolved in DMSO to achieve a 5 mM stock and diluted to a highest concentration at the time of injection of 3 µM. From this 3 µM stock, 4 serial dilutions were generated by 1/3 fold. The vehicle/control used was 0.1% DMSO. Injections were as follows: compounds of interest, oligomycin (1.5 µM), FCCP (1.2 µM), and rotenone/antimycin a (each at 1.0 µM). Following analysis, the cell counts were normalized per 1,000 cells using the Seahorse XF Imaging and Normalization System. Data were visualized with the Wave 2.6.1 software and extrapolated to GraphPad Prism 6. Bioenergetic parameters were extrapolated to the mito-stress test Excel worksheet and data plotted in GraphPad Prism 6. All statistical analysis was done in GraphPad Prism 6 using one way ANOVA.

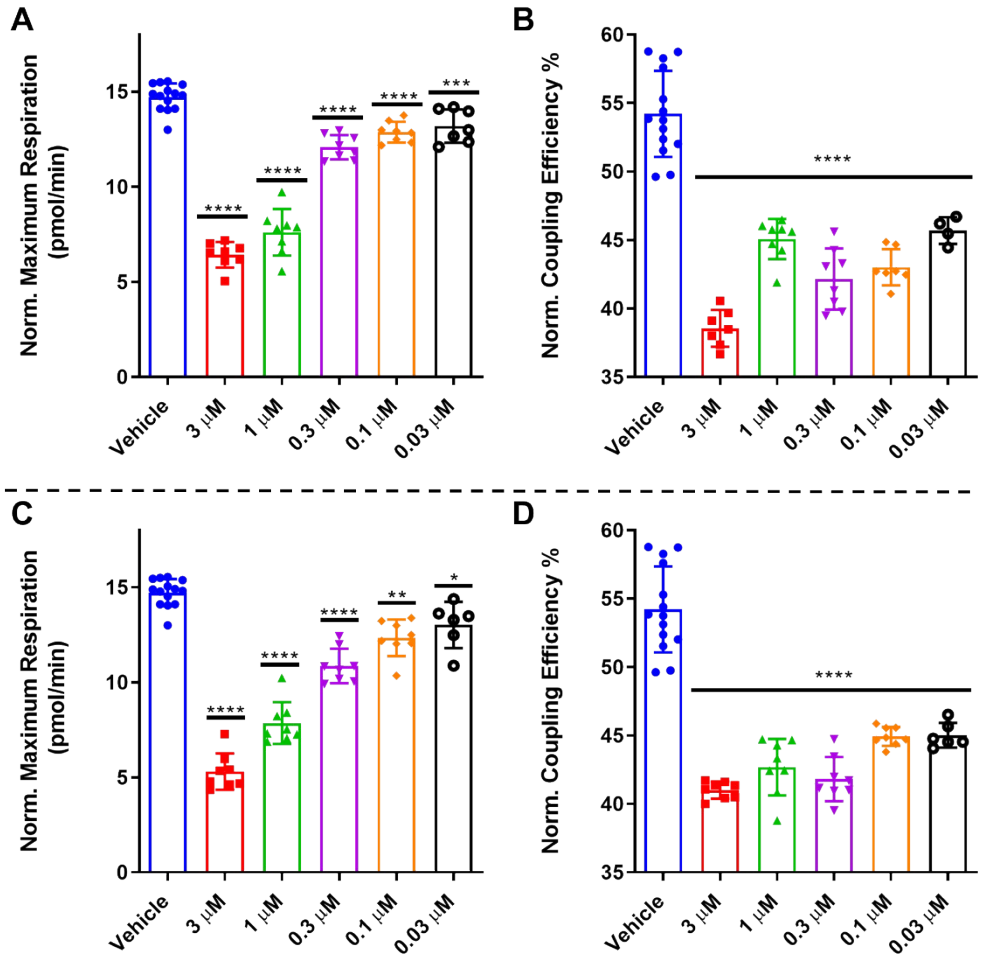

Figure S52. Bioenergetic parameters were extracted from the OCR plot: Maximal Respiration and coupling efficiency for compounds 2 (A-B) and 4 (C-D) on A549 cells. Data in the bar charts are plotted as the mean + s-d. p values were calculated by one way ANOVA using GraphPad Prism 6, * $p < 0.05$, *** $p < 0.001$, **** $p < 0.0001$.

ATP Rate Assay

A549 cells were seeded at a density of 2 x 10^4 cells/well in a 96 well Seahorse XFe plate two days prior to the assay and allowed to adhere. 5 mM stocks of both compounds were prepared in DMSO and the cells treated at the corresponding concentrations. The vehicle/control used was 0.1% DMSO. Injections were as follows: oligomycin (1.5 µM) followed by rotenone/antimycin a (each at 1.0 µM). Following analysis, the cell counts were normalized per 1,000 cells using the Seahorse XF Imaging and Normalization System. Data were visualized with the Wave 2.6.1 software and extrapolated to GraphPad Prism 6. Bioenergetic parameters were extrapolated to the Mito-stress test Excel worksheet and data plotted in GraphPad Prism 6.0. All statistical analysis was done in GraphPad Prism 6 using one way ANOVA.

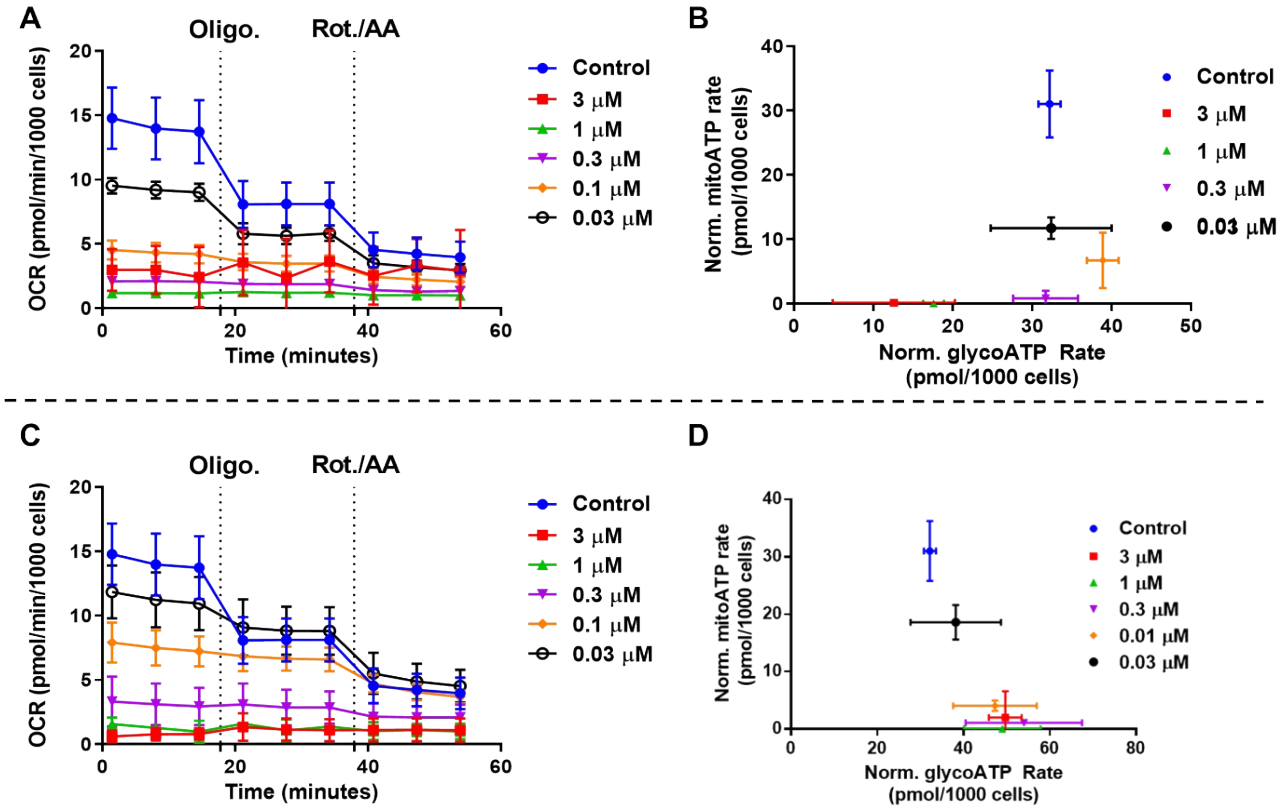

Figure S53. ATP-rate was extracted from the OCR/PER ratio to give contributions of glycolytic and mitochondrial linked ATP for compounds 2 (A-B) and 4 (C-D).

mtROS using MitoSox

5 x 10^5 A549 cells were seeded in 6-well dishes and adhered overnight. The cells were then treated with respective compounds for 24 hours at the IC_{50} and 2x the IC_{50} value. After treatment, the media was removed, washed with PBS (3 x 1 mL) and incubated with 5 µM MitoSox dye for 20 minutes at 37 °C in the dark. The cells were then washed with PBS (3 x 1 mL) and collected via trysinization and suspended in 300 µL of media. The cells were analyzed using FACS, with the PE channel. Cells were gated by live/dead and excluded aggregates. Count = 20,000 gated events per replicate, n = 3. Data were plotted using FlowJo 7.6.5.

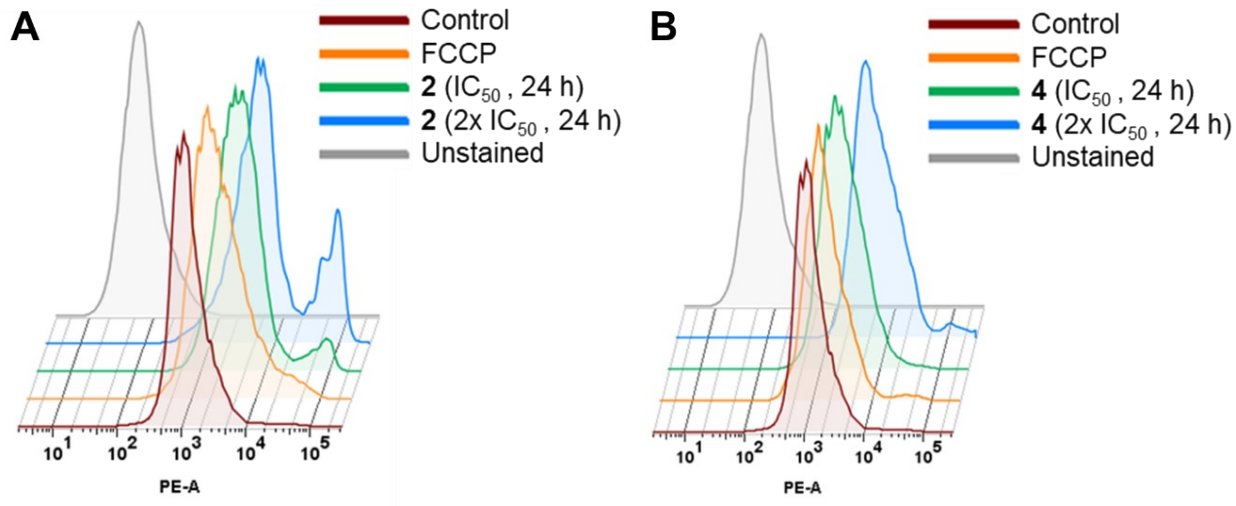

Figure S54. FACS histograms are representative of three individual experiments where A549 cells were treated with compounds **2** and **4** at their IC_{50} and 2x IC_{50} for 24 h, and FCCP was used as positive control.

Mitochondrial Membrane Potential (JC-1)

5 x 10^5 A549 cells were seeded in 6-well dishes and adhered overnight. The cells were then treated with respective compounds for 24 hours at the IC_{50} value. After treatment the cells were washed with PBS (3 x 1 mL) and collected via trypsinization. The cells were suspended in a 1:100 JC-1 solution (diluted with media, Cayman Chemicals) and stained for 30 minutes at 37 °C in the dark. The cells were centrifuged and washed with PBS, suspended in media, and analyzed using FACS (FITC channel for J-monomers, PE channel for J-aggregates. Cells were gated by live/dead and excluded aggregates. Count = 20,000 gated events per replicate, n = 3. Data were plotted using FlowJo 7.6.5.

shRNA signatures assay[17–19]

For the preparation of shRNA viral vectors, phoenix cells (Human Embryonic Kidney 293T) were used for transfection. Phoenix cells were cultivated in DMEM media containing 10% FBS, 1% Pen-Strep-Glutamine. Eight shRNA plasmids GFP-tagged and Ψ viral vector were transfected using the "calcium phosphate" method ($CaCl_2$ stock solution 2 M and Hepes buffer solution). GFP signals were observed after 48 h with a fluorescence microscope (Evos FL auto imaging system from Thermofisher) to confirm the presence of at least 50 % of GFP-positive cell population. Media was changed every 24 h for 48 h before infection of the mice lymphoma cells (Eμ-Myc). Eμ-Myc were cultivated in 1:1 DMEM-IMDM media containing 10% FBS, 1% Pen-Strep-Glutamine and 55 μM of 2-mercaptoethanol. shRNA viral vectors were purified and concentrated (before infection) with polybrene and chondroitin sulfate (80 μg/mL). After centrifugation, the supernatant was removed and viral pellets were re-dissolved in 500 μL of fresh media (DMEM-IMDM-FBS 2.5%-BME 55 μM-1% Pen-Strep-Glu). Eμ-Myc cells were then seeded in 10 cm dishes and 6-well plates at $1x10^5$ cells/mL in media (DMEM-IMDM-FBS 2.5 %-BME 55μM-1 % Pen-Strep-Glu) and infected with purified shRNA viral vectors (volumes vary depending on the shRNA viral vector). The rest of the viral solution (400 μL) was stocked in a 1:1 mixture of glycerol and Eμ-Myc (400 μL; vol total = 800 μL) media and stored at – 20 °C. After 48 h, the supernatant containing the virus was removed after spin-down (500 rpm, 5 min, room temperature) and pellets were washed twice by PBS. Infected Eμ-Myc cells were seeded in 10 cm dishes and infection % (between 10-20% GFP positive cell population, depending on the shRNA viral vector, Figure S16) was determined by flow cytometry (BD Accuri C6 Plus).

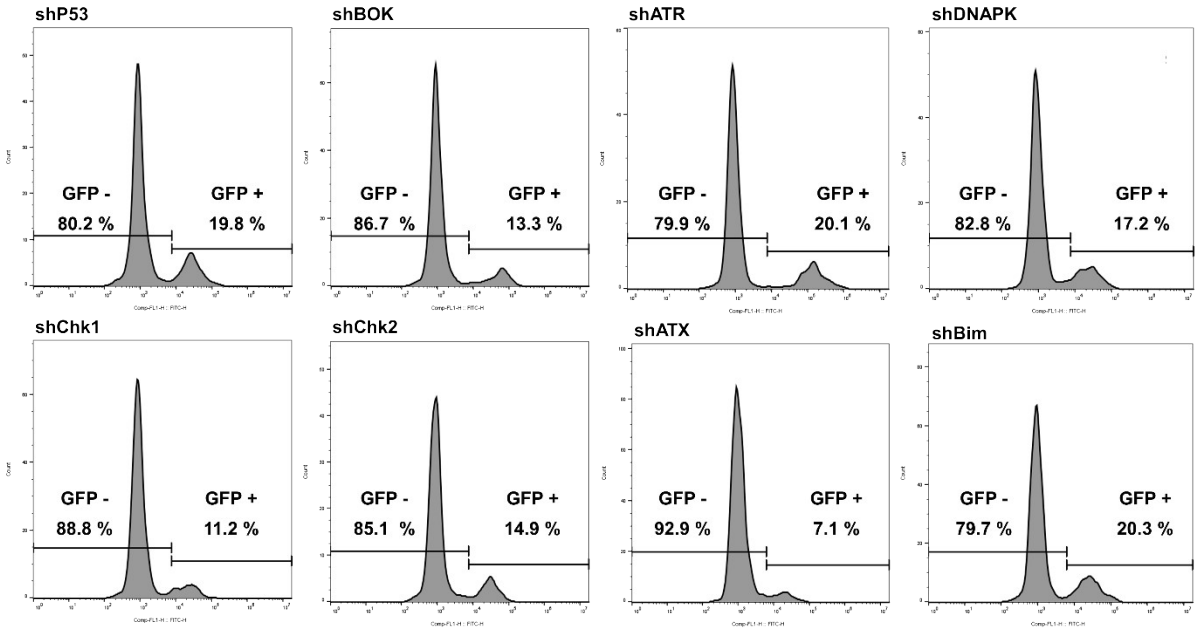

Figure S55. Transfection controls from the shRNA signatures experiment for the eight Eμ-Myc cell lines infected with GFP-tagged shRNAs.

Before the shRNA signatures experiment, IC_{50}, IC_{80} and IC_{90} for 48 h were determined for compounds **1-4**, cisplatin and doxorubicin on wild type Eμ-Myc cell line with propidium iodide as viability marker by flow cytometry. For the shRNA signatures experiments, Eμ-Myc cells were seeded in 10 cm dishes at 10^5 cells/mL and treated at three different at IC_{80}, IC_{85} and IC_{90} for 72 h in triplicate and analyzed by flow cytometry (10^4 events per sample were recorded and each experiment was conducted once at least in triplicate) with propidium iodide (PI) at 10 μg/mL to determine of resistance index (RI). RI were calculated with the following equation (G1 = GFP % of the untreated GFP^+/PI^- population; G2 = GFP % of the treated GFP^+/PI^- population):

$$RI = \frac{G2 - (G1 * G2)}{G1 - (G1 * G2)} \quad \text{(eq. 2)}$$

Classifications are predicted by analysis of $\log_2$RI by K-means and principal component analysis (PCA) with the R program. Cisplatin and doxorubicin were used as positive control and were correctly classified as DNA cross-linking agents and topoisomerases II inhibitors, respectively.

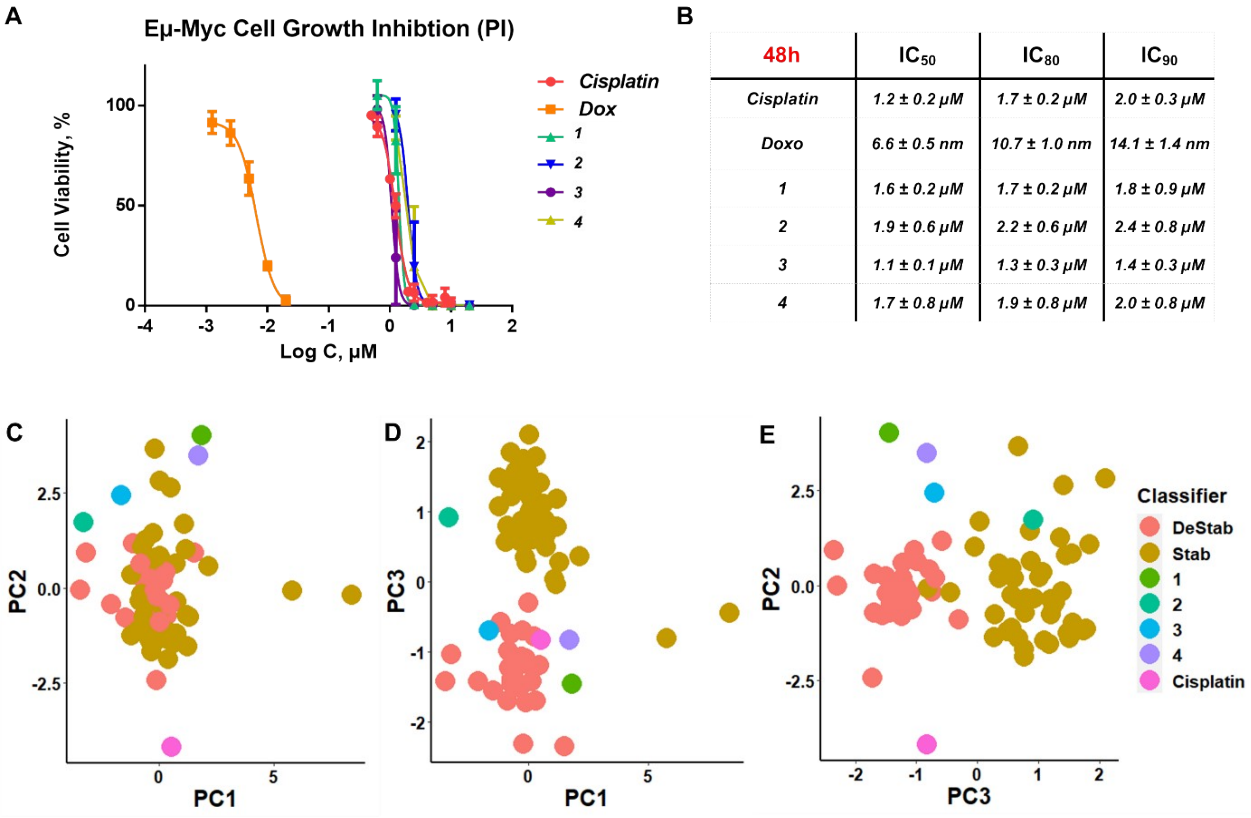

48h	IC_{50}	IC_{80}	IC_{90}
Cisplatin	*1.2 ± 0.2 μM*	*1.7 ± 0.2 μM*	*2.0 ± 0.3 μM*
Doxo	*6.6 ± 0.5 nm*	*10.7 ± 1.0 nm*	*14.1 ± 1.4 nm*
1	*1.6 ± 0.2 μM*	*1.7 ± 0.2 μM*	*1.8 ± 0.9 μM*
2	*1.9 ± 0.6 μM*	*2.2 ± 0.6 μM*	*2.4 ± 0.8 μM*
3	*1.1 ± 0.1 μM*	*1.3 ± 0.3 μM*	*1.4 ± 0.3 μM*
4	*1.7 ± 0.8 μM*	*1.9 ± 0.8 μM*	*2.0 ± 0.8 μM*

Figure S56. A. Determination of IC_{50} for compounds **1-4**, cisplatin and doxorubicin on the Eμ-Myc cell line with propidium iodide as viability marker. C, D and E. PCA plots of log_2RI for Stab (stabilizers or inhibitors of microtubules depolymerization including paclitaxel, taxol and docetaxel), DeStab (destabilizes or inhibitors of microtubules polymerization including vincristine, vinblastine and vinorelbine) and for compounds **1-4** on eight Eμ-myc knockdown cell lines.

Tubulin immunostaining

$2x10^5$ G9pCDH cells per well were seeded on 8-well chambered slide. 24 h later, G9pCDH cells were treated with compounds **2** and **4** at their IC_{50}. Control wells were left untreated. 48 h after seeding, G9pCDH cells were washed with PBS (500 μL), fixed for 30 min with 1% PFA (200 μL/well, from 16% stock solution PFA from Electron Sciences). 200 μL of blocking buffer (1% donkey serum, 0.05% Tween 20) were then added in each well for incubation during 1 h. Cells were incubated with primary antibody in solution in blocking buffer at room temperature overnight. After incubation, cells were rinsed in washing buffer (0.05 % Tween 20, 0.01 % Triton in PBS, pH 7.2) 3 times (500 μL) for 5 min. Secondary antibody in blocking buffer (secondary antibody dilution 1:500, DNA labeling 1:2000 Hoechst) was then incubated with cells for 1 h and then rinsed with washing buffer 5 times for 5 min. Finally, slides were covered with coverslip glass, washing buffer was aspired as much as possible and a drop of glycerol-based mounting medium was added, coverslip was pressed down and excess of medium was aspired. Samples were analyzed using confocal microscope.

Tubulin polymerization assay

The Tubulin Polymerization Assay kit (Cat. # BK006P) was purchased from Cytoskeleton, Inc. and run according to the manufacturer's protocol. Polymerization was initiated by adding 100 μL of 3 mg/mL tubulin in 80 mM PIPES pH 6.9, 0.5 mM EGTA, 2 mM $MgCl_2$, 1 mM GTP, 10% glycerol buffer to a pre-warmed 96 well plate at 37 °C, containing a control, positive control (paclitaxel), negative control (colchicine) and the metal complexes (**2** and **4**). After tubulin addition, absorbance was measured at 340 nm over 60 minutes at 37 °C, determined using a SpectraMax® iD3 microplate reader in kinetic absorbance mode. The experiment was performed in triplicate (mean values are presented). Data were exported and polymerization plotted using Graphpad 6.0 software. Absorbance of metal complexes, paclitaxel and colchicine at 10 mM were measured and subtracted to data.

GILA (growth in low attachment) assay

The GILA (growth in low attachment) assay was used to assess the growth of glioblastoma GSCs G9pCDH and G30pCDH.[20] Patient-derived GSCs expressing the fluorescent GFP protein were dissociated into a single cell suspension, and 2000 cells were seeded into each well of a U-shaped low attachment 96-well plate with the aforementioned supplemented serum-free neurobasal medium. After 24 h of incubation at 37 °C, the compounds (**1** and **3**) were added in serial dilution as for the MTT assay. Before and after adding the compounds, the neurospheres were imaged every 24 h with a Nikon fluorescent microscope and NIS Element software. The fluorescence was quantified by ImageJ software and results are given as the mean and its standard deviation.

***In vivo* experiments**

Mice (n = 5 per group) were injected subcutaneously into the flank region (dorsolateral region) with $2x10^5$ G9pCDH in 50 µL Matrigel. First treatment occurred 18 days after cell implantation, with 5 mg/kg body weight of metal complex (**2** or **4**) in a volume of 25 µL per mice (100 µg from a stock solution of metal complex at 8 mg/mL diluted in 50% solution PBS:*N*-methyl-2-pyrrolidone (NMP) at 4 mg/mL), mice were then treated twice a week for 28 days. The control group was treated similarly with the 50% PBS/NMP solution. The fluorescence was quantified by the LifeScience Caliper software (v4.3). Tumor volume was measured by caliper and calculated according to the following formula:

$$Volume(mm^3) = {[Width(mm)^2 \times Length(mm)]}/{2} \qquad \text{(eq.3)}$$

All animal experiments were performed in compliance with the relevant laws and institutional guidelines. The procedures described in this study were approved by Brigham and Women's Institutional Animal Care and Use Committee (IACUC).

References

[1] Martin A. Bennett and Anthony K. Smith, *J. Chem. Soc., Dalt. Trans* **1974**, *0*, 233–241.

[2] S. W. H. Stahl, *Organometallics* **1990**, *9*, 1876–1881.

[3] R. E. Morris, R. E. Aird, P. Del Socorro Murdoch, H. Chen, J. Cummings, N. D. Hughes, S. Parsons, a. Parkin, G. Boyd, D. I. Jodrell, P. J. Sadler, *J. Med. Chem.* **2001**, *44*, 3616–3621.

[4] A. F. A. Peacock, A. Habtemariam, S. A. Moggach, A. Prescimone, S. Parsons, P. J. Sadler, V. Uni, W. M. Road, E. Eh, *Inorg. Chem.* **2007**, *46*, 2966–2967.

[5] B. Higgins, B. A. DeGraff, J. N. Demas, *Inorg. Chem.* **2005**, *44*, 6662–6669.

[6] A. A. Bhattacharya, T. Grüne, S. Curry, *J. Mol. Biol.* **2000**, *303*, 721–732.

[7] F. Neese, *Wiley Interdiscip. Rev. - Comput. Mol. Sci.* **2012**, *2*, 73–78.

[8] J.-D. Chai, M. Head-Gordon, *Phys. Chem. Chem. Phys.* **2008**, *10*, 6615–20.

[9] F. Weigend, R. Ahlrichs, *Phys. Chem. Chem. Phys.* **2005**, *7*, 3297–3305.

[10] F. Weigend, *Phys. Chem. Chem. Phys.* **2006**, *8*, 1057–65.

[11] E. Van Lenthe, E. J. Baerends, J. G. Snijders, *J. Chem. Phys.* **1993**, *99*, 4597.

[12] C. Peng, H. Schlegel, Bernhard, *Isr. J. Chem.* **1993**, *33*, 449–454.

[13] C. Peng, P. Y. Ayala, H. B. Schlegel, M. J. Frisch, *J. Comput. Chem.* **1996**, *17*, 49–56.

[14] J. Tomasi, B. Mennucci, R. Cammi, *Chem. Rev.* **2005**, *105*, 2999–3093.

[15] M. H. M. Klose, M. Hejl, P. Heffeter, M. A. Jakupec, S. M. Meier-Menches, W. Berger, B. K. Keppler, *Analyst* **2017**, *142*, 2327–2332.

[16] O. Debeir, P. Van Ham, R. Kiss, C. Decaestecker, *IEEE Trans. Med. Imaging* **2005**, *24*, 697–711.

[17] H. Jiang, J. R. Pritchard, R. T. Williams, D. a Lauffenburger, M. T. Hemann, *Nat. Chem. Biol.* **2011**, *7*, 92–100.

[18] J. R. Pritchard, P. M. Bruno, L. A. Gilberta, K. L. Caprona, D. A. Lauffenburger, M. T. Hemann, *Proc. Natl. Acad. Sci. U. S. A.* **2013**, *110*, DOI 10.1073/pnas.1210419110.

[19] J. R. Pritchard, P. M. Bruno, M. T. Hemann, D. A. Lauffenburger, *Mol. Biosyst.* **2013**, *9*, 1604–1619.

[20] G. Berger, K. Grauwet, H. Zhang, A. M. Hussey, M. O. Nowicki, D. I. Wang, E. A. Chiocca, S. E. Lawler, S. J. Lippard, *Cancer Lett.* **2018**, *416*, 138–148.

Author Contributions

M.M. and G.B. conceived and designed the research program. A.I, V.M, M.K. helped for the MTT assays and flow cytometry experiments. J.R.P., H.I. and C.J.M. participated the shRNA experiments, M.O.N. helped for the in vivo experiment. T.R.M. and S.A. performed the in vitro test on mitochondria. The manuscript was written by M.M. and G.B. with contributions from all authors. M.M. prepared all figures**.**